SYNTHESIS AND CHARACTERIZATION OF
PYRENE LABELED COPOLYMERS

SYNTHESIS AND CHARACTERIZATION OF

PYRENE LABELED

POLY(*N*-ISOPROPYLACRYLAMIDE-

CO-*N*-ACRYLOYL-*L*-VALINE) COPOLYMERS

By

MING LI

A Thesis

Submitted to the School of Graduate Studies

in Partial Fulfilment of the Requirements

for the Degree

Master of Science

McMaster University

Master of Science (1997)   McMASTER UNIVERSITY
(Chemistry)   Hamilton, Ontario, Canada

TITLE: Synthesis and Characterization of of Pyrene Labeled
                (*N*-isopropylacrylamide-*co*-*N*-acryloyl-*L*-valine) Copolymers

AUTHOR: Ming Li, (MSc, Jilin University, Changchun, P. R. China)

SUPERVISOR: Professor F. M. Winnik

NUMBER OF   Xiii, 106
PAGES:

ABSTRACT

Pyrenebutylamide-labeled   poly(*N*-isopropylacrylamide-*co*-*N*-acryloyl-*L*-valine)

copolymers have been prepared by two different methods and their physicochemical

properties have been compared.   One sample was prepared via copolymerization of *N*-

isopropylacrylamide   (NIPAM),   and   *N*-acryloyl-valine   (NAV)   with   *N*-[4-(1-

pyrenyl)butylacrylamide], the other by post-modification of poly(*N*-isopropylacrylamide-

co-*N*-acryloyl-*L*-valine-*co*-*N*-acryloxysuccinimide)   copolymer   with   pyrenebutylamine

hydrochloride.   The polymers were characterized by 1H NMR and FTIR spectroscopy,

Differential scanning calorimetry and light Scattering.   Though the use of fluorescence

spectroscopy several differences between the two types of copolymers were detected.   By

comparing the extent of pyrene excimer emission and pyrene monomer emission from

solutions of the two polymers, it was concluded that the copolymer obtained by direct

copolymerization (method 1) had an inherent "blocky" microstructure, while the

copolymers obtained by the post-modification route presented a more random

microstructure.   Intrapolymeric interaction exists in solutions of low copolymer

concentrations.   At higher concentrations both inter- and intrapolymeric interactions

coexist.   The presence of a number carboxylic groups in the PNIPAM chain significantly

modifies the conformation properties of the copolymers, compared to poly(*N*-

isopropylacrylamide).   The copolymers contract and expand in response to external

conditions such as pH and temperature.   Their Lower critical solution temperature

(LCST) changes with pH.

The interactions between polymers and fluorescence quenchers were investigated. The quenching results reveal that hydrophilic cationic quenchers interact strongly with the randomly labeled-copolymer. Hydrophobic cationic species interact strongly with "blocky" pyrene labeled copolymer. Anionic quencher interacts quite weakly with both copolymers owing to electrostatic repulsion.

ACKNOWLEDGEMENTS

TABLE OF CONTENTS

LIST OF FIGURES

LIST OF TABLES

LIST OF SYNTHETIC SCHEMES

LIST OF DIAGRAMS

1.0 Introduction

In the past two decades, intelligent polymers have attracted extensive attention for their potential applications in such diverse fields as medicine, biotechnology, industry and environmental problems.[1-8] These polymer materials can be tailored to undergo reversible phase transition in response to a variety of external physico-chemical stimuli (e.g. temperature, pH, oxidative-reductive reactions and electrical field), biochemical signals such as enzymes (e.g. GOD glucose oxidase) that act as signal transducers in glucose-sensitive insulin releasing systems,[5-7] or nature of a solvent. However, most of the polymers studied previously are responsive to only one stimulus. For example, poly(4-vinylpyridine) grafted on a microfiltration membrane is responsive to the change in pH[8]. Thus, exploring the synthesis and properties of modified poly(N-isopropylacrylamide) (PNIPAM), a typical representative polymer, which can respond to more than one kind of stimulus, remains a challenging target to be achieved. The objectives of this thesis were to study one family of polymers based on PNIPAM, which responds to two types of triggers: temperature and pH.

1.1 PNIPAM and Modified PNIPAM

The first preparation of PNIPAM was reported in 1957,[9, 10] however, it is only in the past decade that PNIPAM has become an important water-soluble polymer. The main impetus for studying PNIPAM as a basic material is its prominent thermo-sensitive behavior in aqueous media. PNIPAM has been used in many forms including solutions,

macroscopic gels, microgels, latexes, thin films, membranes, coatings and fibers.[11] Its Lower Critical Solution Temperature (LCST) approaches human body temperature. It is this property that makes the polymer a useful thermoresponsible material for pharmaceutical and biomedical applications.[12-15]

The copolymers of PNIPAM with monomers containing carboxylic groups have been explored as multiple stimuli-responsive polymers.[2,3] It is expected that the copolymer conformation responds to the change of both pH and temperature. The LCST of copolymers can be changed by varying the chemical structure and application conditions (e.g. pH). The properties of polyelectrolytes are greatly affected by the addition of simple salts such as sodium chloride.[1] The polarity and shape of ionizable polymer chains changes considerably with the degree of ionization. The ionization of the carboxylic groups in the copolymer chains give rise to electrostatic repulsion along the chain and result in the expansion of the originally coiled molecule. The protonated form of the polymer in water should be assumed to be a compact coil conformation when short-range attractive interactions outweigh electrostatic forces. In most cases, the coil dimension regularly decreases over the whole range of the degree of protonation due to the neutralization of the COO^- groups and accompanying electrostatic force.[58] Hydrophobic groups on the polymers may provide a further chain contraction, and in some cases the polymer precipitates because the hydrophobic moieties overcome the hydrophilic quality of the carboxyl groups at a relative low charge density.

F. M. Winnik et al[16,17] have reported the solution properties of PNIPAM and

hydrophobically modified PNIPAM (*N*-alkylacrylamides). The solubility of PNIPAM in water depends on temperature. The mechanism of phase separation and the shrinking of molecular coils in solution were monitored by fluorescence spectroscopy. The results of hydrophobically modified PNIPAM revealed the existence of polymeric micelles below the LCST in aqueous solution while the hydrophobic substituents are randomly distributed among the collapsed and aggregated PNIPAM chains above the LCST.

S. W. Kim and coworkers[18-22] reported the effect of hydrophilicity and ionization of comonomer on the LCST of PNIPAM copolymers. The copolymers were prepared with cationic, anionic, hydrophilic or hydrophobic comonomers. The changes in the LCST of those copolymers were caused by changes in overall hydrophilicity of the polymer and were not caused by a direct influence of hydrophilicity or charge of comonomer on the structuring of water around hydrophobic groups.

M. Casolaro[2, 23 24] reported the synthesis and protonation thermodynamics of poly(*N*-isopropylacrylamide-*co*-*N*-acryloyl-*L*-valine), poly(*N*-isopropylacrylamide-*co*-*N*-acryloyl-*L*-leucine) and methacrylic acid derivatives containing *L*-valine and *L*-leucine residues (scheme 1). These series of copolymers were prepared by free radical copolymerization in organic solvents. Thermodynamic studies show that the basicity constants (log K) for protonation of the carboxylic groups decreased linearly with the degree of protonation α, until a critical value of α is reached, where log K increased. Calorimetric data revealed a sharp endothermicity superimposed on the protonation of carboxylic groups. The data was explained in terms of hydrophobic interactions

3

outweighing the electrostatic repulsion above the critical α value. The whole protonation

process is entropically driven and leads to the collapse of the macromolecular coils which

results in the release of a large number of water molecules structured around the polymer.

$$(CH_2-CH)_m-(CH_2-CH)_n-$$

C=O C=O
| |
NH NH   x=0, valine
| |
CHCOOH CH(CH₃)₂   x=1, leucine
|
(CH₂)ₓ
|
CH(CH₃)₂
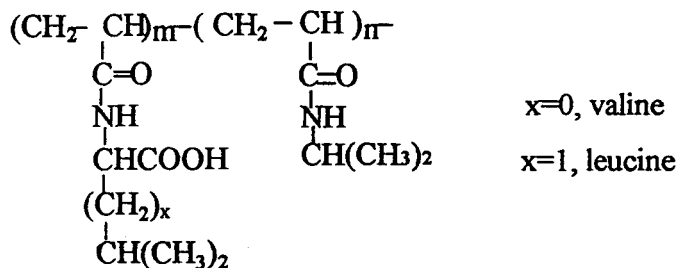
Scheme 1   chemical structure of poly(*N*-isopropylacrylamide-co-*N*-acryloyl-*L*-valine) and poly(*N*-isopropylacrylamide-co-*N*-acryloyl-*L*-leucine)

A. S. Hoffman and coworkers[25, 26] recently synthesized comb-type graft

copolymers of PNIPAM-g-poly (acrylic acid, AAc, scheme 2). These copolymers

represent a new family of 'hybrid intelligent' materials. The graft or block copolymers

could become even more 'intelligent' in combination with various biomolecules.

Applications of these copolymer-biomolecule systems include drug delivery, diagnostics,

separations, cell culture and bioreactions.

$$-(CH_2-CH)_m-(CH_2-CH)_n-$$
$$|\qquad\qquad\quad|$$
$$C=O\qquad\quad C=O$$
$$|\qquad\qquad\quad|$$
$$NH\qquad\quad OH$$
$$|$$
$$CH_2$$
$$|$$
$$CH_2$$
$$|$$
$$S$$
$$|$$
$$(CH_2$$
$$|$$
$$CH)_x$$
$$|$$
$$C=O$$
$$|$$
$$NH$$
$$|$$
$$CH(CH_3)_2$$
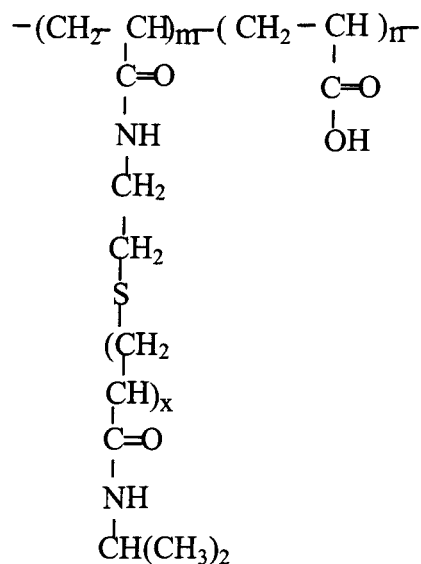
scheme 2: Chemical structure of PNIPAM-g-PAAc

Polymer chain extension and contraction can be enhanced by the construction of a three-dimensional polymer network in hydrogels. T. Okano and coworkers[27] have reported the swelling/deswelling behavior of thermosensitive comb-type grafted neutral PNIPAM hydrogels. These gels demonstrate rapid dehydration and hydration in response to a small temperature change in an aqueous environment. A. Gutowska and S. W.Kim[28-30] synthesized the PNIPAM/AAc crosslinked copolymers with 2 mol% AAc in order to apply these thermosensitive polymer gels for the entrapment of insulin secreting islets of Langerhans in an immunoprotecting pouch. This copolymer exhibited a swelling transition at 37 °C (pH 7.4) and fast swelling/deswelling. Poly(NIPAM/AAc) copolymer entrapped almost 100% of the islets, whereas the PNIPAM homopolymer entrapped only 50% of cells. In addition, the islets entrapped within the

5

poly(NIPAM/AAc) gel matrix demonstrated a prolonged viability in vitro.

1.2 Background

1.2.1 Polymer Conformation in Solution

The conformation (shape) of a polymer molecule in dilute solution is mainly determined by its chemical structure. Since most polymers have relatively flexible backbones, they tend to be highly coiled and can be represented as random coils. However, as the backbone becomes stiffer, the chains begin to adopt a more elongated worm-like shape and ultimately become rod-like.[31] For example, polyelectrolytes ionize in water or other strong polar solvents to form ionized polymers. The electrostatic repulsion of the fixed charges on a flexible polymer chains results in an expansion of the macromolecular coil, but expansion is also countered by the retractive force due to the rubberlike elasticity of the chain. The addition of salt to the solution changes the ionic strength of the medium, and produces a shielding effect for the fixed charges. The interaction of counterions with the ionizable polymer modifies the electrostatic forces between the fixed charges and the shape of the ionizable polymer.

1.2.2 Polymer-Polymer Complexes

The association phenomena of more than two different macromolecular chains in solution is caused by non-covalent bonding. The obtained associates are generally called "intermacromolecular (interpolymer) complexes" or "polymer-polymer complexes".[9] In recent years, there has been a growing interest in the study of polymer-polymer

complexation of structurally complementary synthetic polymers for several reasons. Firstly, polymer-polymer complexation is closely related to many life processes, such as the replication of DNA. As a simple model of biopolymers, the study of the polymer-polymer complexation with the synthetic polymers help one to understand the mechanism of similar processes between biopolymer in living cells. Secondly, polymer-polymer complexation offers a new and effective way to develop polymer materials with high performances.[9] The final properties of polymer materials not only depend on first-order structures but also on second or higher-order structures. Furthermore, these macromolecules may aggregate due to non-covalent bonding. This aggregation phenomenon can be observed on the macroscopic level as phase separation, such as precipitation, gelation, coacervation, and emulsion. The regularities in the orientation of the macromolecular chains are changed from random mixing states to a more specific higher-order structure according to the above mentioned order.

Non-covalent bonding is mainly classified into electrostatic interaction, hydrogen-bonding, van der Waals, charge transfer, and hydrophobic interaction (Table 1).

Tabel 1 Non-covalent Interaction and Species

non-covalent bonding	interaction species
electrostatic	charged species
van der Waals	molecules with permanent or induced dipoles
charge-transfer	electron donor and acceptor
hydrophobic interaction	hydrocarbons in aqueous medium

One interesting class of polymer-polymer complexes (polymer associates) is hydrogen-bonding complexes. Hydrogen-bonding complexes are formed between polymers bearing proton-accepting units and proton-donating units. Most of the polymer-polymer complexes in biological systems are governed through hydrogen bonds. However, complexes between synthetic polymers reported in the literature are limited to a few polymer systems consisting of proton-donor and proton-acceptor, for example, poly(carboxylic acid)-poly(ethylene oxide)(PEO), [33] -poly(vinyl alcohol) (PVA)[34] and -poly-(N-vinyl-2-pyrrolidone) (PVPo).[35] P. Somasundaran et al[36-39] recently reported the complexation of poly(acrylic acid) with poly(acrylamide) and hydrolyzed poly(acrylamide). C. W. Frank and his coworkers[40] reported complexation of poly(methacrylic acid) or poly(acrylic acid) with poly(oxyethylene) and poly(N,N-dimethyl-acrylamide-co-acrylamide) in water. We observed the complexes that occurred between same type of copolymers (inter- or intra-molecules) in acidic conditions in this thesis.

Proton-accepting polymers and proton-donating polymers typically interact with each other in aqueous medium almost stoichiometrically. The complex formation is affected by temperature, polymer structure, polymer concentration and nature of solvent. With the poly(carboxylic acid) system, the complexation strongly depends on the pH of the solution, i.e. the degree of dissociation of poly(carboxylic acid). In this kind of polymer, hydrogen bonding complexes can only be formed in solutions below a "critical pH", above this pH no complex can be formed because of the dissociation of the carboxyl group. The complexation mechanism involving hydrogen bonds is described by the following equations (e.g. PMMA and PEO system)

below the critical pH

above the critical pH
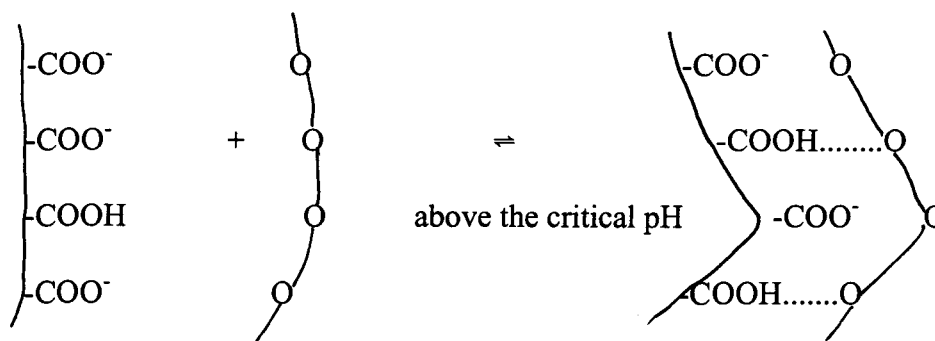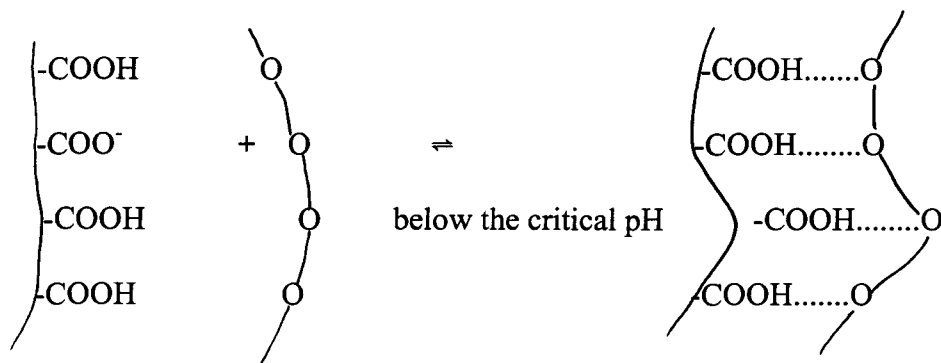
The existence of a certain number of protonated carboxylic groups is necessary for PMMA and PEO to form a stable complex through hydrogen bonds. If this condition is satisfied at the "critical pH", a stable complex will be formed reversibly. The formation of complexes containing hydrogen bonds can be detected by NMR, IR and fluorescence, ect. Q. Wang and coworker studied complexation between poly(acrylonitril-acrylamide-acrylic acid)/ poly(vinyl alcohol) by IR and DSC.[41] The fluorescent methods based on the photophysical and photochemical properties of a covalently bonded fluorescent probe to the polymer have been found to be both sensitive and informative for the investigation of interpolymer complexation via hydrogen bonding. W. Frank, N.J. Turro[40] and P. Somasundaran et al[36-39] investigated the intermacromolecular complexes by using fluorescence spectroscopy.

1.3 Microscopic Characteristics of Polymer with Fluorescence Techniques

Photophysical techniques are powerful tools to extensively study the microstructure of polymeric systems from fundamental to practical perspectives. The application of photophysical properties in macromolecule studies is to introduce luminescent probes to polymer systems for investigating segmental motions, microstructures and microenvironments. These methods can be either static or dynamic (time-resolved, or transient). One can observe emissive light from fluorescence emission, fluorescence anisotropy, excimer fluorescence, exciplex fluorescence and fluorescence quenching sources. The advantage of luminescent chromophore methods

can be summarized by their high sensitivity and nondestructiveness; they provide

information on interactions over a wide range of radii (a few to 100 Å) and information

about a wide range of time ($>10^{-3}$ sec). The emission from different chromophores gives

different types of information. K. Horie et al[42] classified fluorescent chromophores into

three categories based on the feed information from emission: the microenvironment

probes, microstructure probe and segmental motion probes. The microenvironment

probes (usually hydrophobic probes), such as pyrene, are those whose emission

intensities or maximum emission wavelengths are sensitive to the properties of the local

microenvironments such as microviscosity, micropolarity and free volume. The

microenvironments around the probes directly affect the electron-transfer process and

energy distribution of the excited state of the probes. A probe which has a charge-

transfer (CT) complex., or a twisted intramolecular charge transfer (TICT) process, is a

typical example of the microenvironment probes, such as amino-naphthalenesulfonate.[43]

The dansyl group as a fluorescence probe has been used widely to investigate both

microstructure and segmental motion of polymer systems in bulk solution.[44]

1. 3. 1 Luminescence Fundamentals and Method

Luminescence is the process in which a molecule in an electronically excited state

returns to the ground state by the emission of a photon. Molecules may return to the

ground state either by non-radiative or radiative (luminescence) processes. A Jablonski

energy-level diagram (Diagram 1) effectively illustrates the characteristics of molecular

electronic states. In the singlet state (denoted by S. vibrational energy levels denoted by

0, 1 ,2, etc.), all electrons are spin-paired, and the overall spin quantum number of the

molecule is zero. In the triplet excited states (denoted by T), one electron has reversed its

spin to create two unpaired electrons, and the molecule has a spin quantum number equal

to one. At normal temperatures and under equilibrium conditions, nearly all molecules

exist in the lowest energy vibration level of the ground electronic state (S_0). However,

absorption of light (hv) from the visible or ultraviolet region of the spectrum may

promote molecules to excited electronic states. In general, fluorescence occurs upon a

radiative transition from an excited singlet state to the ground singlet state (while a

radiation transition from an excited triplet state to the ground singlet state corresponds to

phosphorescence).

Diagram 1 Representative Joblonski Energy Level Diagram
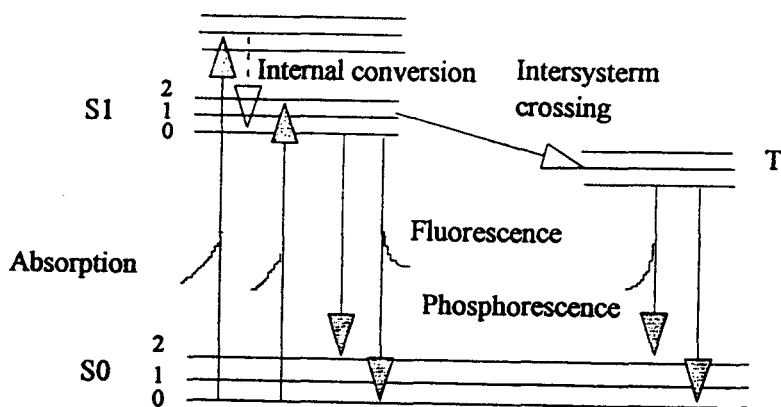
Two approaches are possible in applying fluorescence techniques to the study of

polymer solutions. I) In probe experiments a fluorescent dye is simply dissolved in the solution. This type of experiment is useful if the dye binds to the polymer. II) The polymer is labeled by covalently attaching the dye. The labeled-polymer experiments are often more informative because they report spectroscopic phenomena from the polymer's perspective.

1. 3. 2 Excimer Fluorescence

The concept and photophysical properties of excimer fluorescence from aromatic molecules was first discussed in detail by Birks in 1970.[45] An excimer is an excited state complex that is formed between two identical species, one of which is in the excited state and the other in the ground state. Pyrene, as one of the most commonly used probes, is an excellent excimer probe to investigate polymer properties. The pyrene excimer is a dimer which is associated in an electronically excited state and which is dissociated in its ground state. Pyrene excimer emission arises from a 'sandwich structure' of two pyrene molecules in close proximity. The formation of a pyrene excimer requires the encounter of an electronically excited pyrene with a second pyrene molecule in its ground electronic state.

If the two pyrenes are sufficiently far away when light is absorbed, then the excitation will be localized on one of them. This excited pyrene will give rise to the monomer emission. The observation of excimer emission indicates that a diffusive encounter between the pyrenes has occurred. There are also instances where an excimer-like (dimer) emission is observed; this formation may occur by two different mechanisms. Under normal circumstances, the distinction between static and dynamic excimer is that

13

one can observe the growth of the excimer emission in a time-resolved experiment for "dynamic excimer", but one can not observe the growth of excimer emission in the same experiment for the "static excimer".

Diagram 2   Pyrene Excimer Formation Mechanism

1) Dynamic

$$Py \longrightarrow Py^* + Py \longrightarrow Py\text{-}Py^*$$

$$\downarrow \qquad\qquad \downarrow$$

$$Py \qquad\qquad\qquad Py\text{-}Py$$

(Monomer emisson)   (Excimer emission)

2) Static

$$Py \longrightarrow Py^* + Py \longrightarrow Py\text{-}Py^* \longleftarrow Py\text{-}Py$$

$$\downarrow \qquad\qquad \downarrow$$

$$Py \qquad\qquad Py\text{-}Py$$

(Monomer emission)   (Excimer emission)
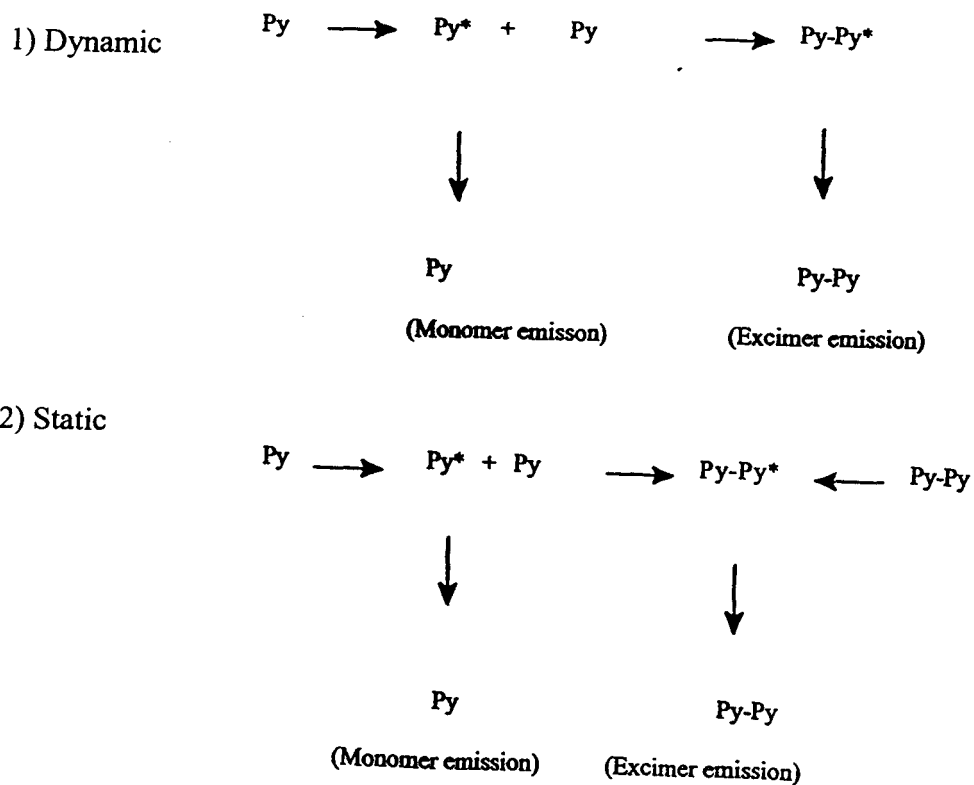
H. G. Schild and D. T. Tirrell [46] reported pyrene-labeled PNIPAM and

14

hydrophobically modified PNIPAM. Incorporation of more than 1.5 % (mol) of N-hexadecylacrylamide(HDAM) renders the copolymers insoluble in water at room temperature. Their Nonradiative Energy Transfer (NRET) studies indicates that no energy transfer from fluorene-labeled PNIPAM to free pyrene or to PNIPAM-bound pyrene takes place in mixed aqueous solutions at 24.5 °C.

Winnik et al.[16, 17] have synthesized pyrene-labeled PNIPAM and hydrophobically modified PNIPAM. They monitored the pyrene excimer fluorescence intensities in water and in methanol. A low excimer fluorescence intensity in methanol was observed, indicating a randomly coiled polymer chain. However, the excimer fluorescence intensity in water was very high, suggesting the association of polymer-polymer chains. The addition of surfactant to the hydrophobically modified polymer solution disrupts the polymeric micelles, thus one could observe a decrease of the excimer intensity.

Frank et al[39] used pyrene excimers to study the complexation of polyacids such as PAA and PMAA with PEO. The addition of PMAA to pyrene end-labeled PEG greatly reduced the ratio of excimer to monomer intensity, indicating a decrease in the intramolecular mobility due to complexation.

C. L. McCormick et al [47, 48] reported the synthesis and solution properties of acrylamido copolymers with pyrenesulfonamide fluorescent labels. The labeled copolymer was prepared by microheterogeneous surfactant techniques. This polymer exhibits a the intermolecular associative behavior in an aqueous media, as demonstrated by rheological and steady-state fluorescence studies. Their surfactant techniques result in

the blocky label being distributed along the copolymer chains, which show large excimer emission.

A pyrene probe not only can reveal information on the microstructure of the polymer systems with its excimer fluorescence, but also can provide information on the local microenvironment in terms of the monomer emission intensity by using the ratio I_1/I_3, for various vibronic fine structure. In view of the extensive information offered by photophysical properties of pyrene groups, pyrene probe technique is one of the most successful, and frequently used methods for the measurement of a variety of microscopic characteristics of polymers in solution. Therefore, the pyrenyl probe was utilized in our system to monitor the conformational changes, microenvironmental changes and the interaction occuring between the copolymers.

1.4 Potential Application of the Copolymer

The intelligent membrane device (Chemical valve) was successfully created by M. Casolaro and co-workers.[49] The multiple stimuli-responsive copolymers (NAV copolymer) were grafted onto the surface of a porous cellulose membrane or polyurethane film. Expansion and contraction of the graft polymer chains, which depend on the change of solution pH in the permeate, give rise to a significant conformational change in the grafted polymer. In this change, the extended graft-polymer chains are brought back to collapsed coil conformation (Scheme2). The valve effect observed with the ultrafiltration membrane occurs over the pH range from 3.5 to 4.4, especially in the narrow pH range of

16

4.1 to 4.4. In this range, the water flow-rate varied more than 2-fold. As a potential

application of this hydrophilic PNIPAM, it may be able to be made into a magnetic

material.

Scheme 3   Principle of Chemical Valve
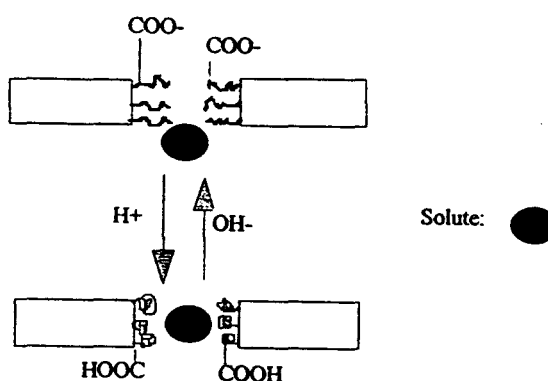
1.5 Objectives

Our research focuses on pyrene labeled PNIPAM materials modified by

carboxylic groups (with both hydrophobic and hydrophilic characteristics). These

copolymers are responsive to external temperature and pH. The first target of the project

was to synthesize and characterize of pyrene chromophore and copolymers. The second

target was to study the polymer solution properties through fluorescence and quenching

techniques to understand the hydrophilically modified PNIPAM microscopic behavior,

and the relationship between the micro- and macroscopic behavior. The third target was

17

to provide basic informations for the preparation of magnetic materials by using this hydrophilic PNIPAM.

2. Experiments

2.1 Materials

N-Isopropylacrylamide (Eastman Kodak Company) was recrystallized twice from toluene/hexane (1/1, v/v). Azobisisobutyronitrile (AIBN) (Dupont) was recrystallized from methanol. L-Valine (99%), 4-(1-pyrenyl)butyric acid (97%), and acryloyl chloride were purchased from Aldrich Chemical Co. and used without further purification. Oxaloyl chloride from Sigma Chemical Co. Lithium aluminum hydride (97%) from Fluka. Tetrahydrofuran (Caledon) was distilled from sodium/ benzophenone before use. Water was deionized with a NANOpure water purification system. Other chemicals were bought either from Caledon Lab. Ltd. or BDH and used as received unless stated otherwise. Buffers were prepared from 0.1 M glycine and 0.1 M HCl/or 0.1 M NaOH, or 0.1 M citric acid and 0.2 M Na_2HPO_4. The ionic strength of both buffers was 100 mM NaCl.

2.2 Instruments

^{1}H NMR spectra were recorded with a Bruker AC-200 spectrometer. Spectra were measured in $CDCl_3$, D_2O, DMSO or a mixture of $CDCl_3$ and DMSO as solvent. Chemical shifts are reported in ppm, downfield relative to the solvent. IR spectra were obtained with a Bio-Rad FTS-40 FTIR spectrometer, samples were prepared as KBr pellets. The bands are reported in wave numbers (cm^{-1}).

Titration were performed with a Tanager automated titrator (Tanager Scientific

system Inc.) equipped with TANA 58-2 software. A digital pH potentiometer was equipped with a electrode and a reference electrode and connected to a computer and piston burette.

Gel permeation chromatography (GPC) was performed on a instrument equipped with a Waters 510 HPLC pump, coupled with Waters 410 differential refractometer and Water 486 tunable absorbance detector. Viscosities were measured with an Ubbelohde Viscometer (150 K660) at 20.0 C, 0.1 M NaCl aqueous as solvent. Mark-Houwink-Sakurada coefficients were used PNIPAM's at 20 °C (η=0.11×Mw$^{0.51}$ cm^3/g)[50a]

UV spectra were recorded with a Hewlett-Packard 8452 Photodiode Array spectrophotometer, equipped with a Hewlett-Packard 89090A temperature controller, operated through HP ChemStation Windows-based software.

Light Scattering data were acquired using a Brookhaven Instrument Corp. Model BI9000AT correlator equipped with a Lexel Laser (λ=514 nm) with the scattering angle at 90°. The temperature was set at 25°C.

Fluorescence spectra were recorded on a SPEX Fluorolog 212 spectrometer equipped with water-jacketed cell holder controlled by a Neslab circulating bath and a DM 3300F data system.

Differential scanning calorimetry (DSC) mearsurement were performed on a DSC 2910 instrument equipped with a standard DSC cell and a Thermal Analyst 2100 systems utility program.

20

Aqueous samples were freeze-dried using a benchtop 3L Lyophilizer.

2.3 Monomer syntheses

2.3.1 Synthesis of *N*-Acryloyl-*L*-Valine (NAV)

2.0 g (0.05mol) of sodium hydroxide, 2.92g (0.025mol) *L*-Valine and a trace amount of 2,6-di-tert-butyl-4-methyl-phenol were dissolved in 10 ml of doubly distilled water (scheme 3a). The solution was mixed with magnetic stirring under nitrogen for 0.5 hour. Then, 3 ml (0.03mol) acryloyl chloride was added dropwise into the solution over 30 minutes and the reaction mixture was kept at 0°C for another two hours and stirred at room temperature overnight. Finally, 30 ml of concentrated hydrochloric acid was added into the solution (pH=1) to precipitate NAV. The sticky solid was triturated with acetone (ca.15 ml), filtered. The monomer (NAV) was isolated by filtration as a white powder to yield 2.18g(75 %). ^{1}H NMR (d_6-DMSO, ppm): 0.89 (m, 6H, H_a); 2.18 (m, 1H, H_b); 4.20 (m, 1H, H_c); 5.75 (d, 1H, H_e); 6.26 (dd, 1H, H_f); 6.46 (dd, 1H, H_f); 8.3 (s, 1H, NH). IR (the frequency of main functional groups, cm^{-1}): 3445 (OH free stretch band), 3356 (NH stretch band), 2800-3000 (CH_2 stretch bands); 1730 (C=O stretch of acid); 1653 (C=O stretch of amido); 1540 (NH stretch of amido); 1620 (C=C); 1465 (CH_3); 1230; (C-O stretch and OH bend of COOH group); 986 (CH_2 bend of CH_2=CH_2 group).

2.3.2 Synthesis of N-[4-(1-pyrenyl)butyl-acryloylamide]

2.3.2.1 Preparation of N-[4-(1-pyrenyl)butylamine) hydrochloride

A solution of 4-(1-pyrenyl)butyric acid (1.25g, 4.35 mol, compound 1) in 25.5 ml of benzene/ DMF (50/1, v/v) was refluxed with oxaloyl chloride (1ml. 11mmol) for 2 hours and then stirred at room temperature overnight. The crude acid was isolated by removing the solvent under vacuum. The residue was dissolved in a mixture of 25 ml of methylene chloride and 4 ml triethylamine. An aqueous ammonium hydroxide solution (10 ml, 28% w/w) was dropped into this solution. The resulting solution was stirred for 20 hours at room temperature. Evaporation of the solvent followed by crystallization with ethanol yielded 1.22g of crude amide (compound 2). Compound 2 (1.22g) suspended in 25 ml of freshly dried THF was dropped into 50 ml of THF containing 1 g of $LiAlH_4$. The mixture was stirred 48 hours at 50°C. It was cooled to room temperature. Excess $LiAlH_4$ was quenched by addition ice-water. The mixture was extracted three times with ether, the ether phase was washed twice with water and removed by rotary evaporator to yield 1 g of a yellowlish solid (compound 3). It was dissolved in methanol, and precipitated by adding concentrated hydrochloride acid. The precipitate was recrystallized from methanol to yield 0.4 g of a grey solid (compound 4). ^1H NMR (DMSO/CDCl$_3$, 1/9, v/v) 7.95 (m, 9H., Ar-H); 3.53 (t, 2H, H$_4$, J=7.16 21Hz); 3.24 (t, 2H, H$_1$, J=7.73Hz); 1.79 (p, 2H, H$_3$, J=3.8, 7.79 Hz); 1.63 (p, 2H, H$_2$, J=3.8, 7.10Hz). IR(cm^{-1}): 1601, 1458, 841, 800.

2.3.2.2 Compound 5: N-[4-(1-pyrenyl)butyl]-acryloylamide

0.4g (1.3 mmol) of compound 4, 0.8 ml (5.7 mmol) triethylamine and a trace

amount of 2,6-d-tert-butyl-4-methyl-phenol were dissolved in dried methylene chloride (40 ml). To this solution 0.2 ml (2.5 mmol) of acryloyl chloride (dissolved in 2ml of methylene chloride) was added dropwised at 0 ° C. The solution was stirred overnight at room temperature. It was washed with 0.1 N HCl, saturated Na_2CO_3 aqueous solution, water, the organic layer was dried with $MgSO_4$. Evaporation of the solvent by rotary evaporator yielded 0.12 g of compound 5, which was purified by column chromatography (silica gel), eluted with ether/ethyl acetate, 5/1. ^1H NMR ($CDCl_3$, ppm): 8.01 (m, Ar-H); 5.8 (d, H); 6.11(dd H); 6.33 (d, H); 4.22(t, H_4); 3.37(t, H_1); 1.87 (m, H_3); 1.65 (m, H_2). IR (cm $^{-1}$): 1665, 1620, 1547, 1458, 977, 840, UV (methanol) λmax 234, 242, 312, 336, 342 nm.

2.4 Synthesis of copolymers

2.4.1 Sythesis of unlabeled copolymer (PNIPAM/NAV)

A copolymer of poly(NIPAM-*and*-*N*-acryloyl-*L*-valine) (PNIPAM/NAV) was obtained by free radical polymerization. NAV (0.568 g, 3.3 mmol) and NIPAM (0.758g, 6.7 mmol) were dissolved in 15 ml dioxane. AIBN(21.3mg), dissolved in 2 ml dioxane, was injected into the solution preheated to 60° C and purged by a magnetic stirrer under a nitrogen atmosphere. The solution was stirred at 60 °C for 20 h. The solution was cooled to room temperature. The polymer was isolated by precipitation into anhydrous ethyl ether. The copolymer was further purified by two reprecipitations from methanol into ether, to yield 1.0 g copolymer. ^1H NMR (D_2O, ppm): 0.841, (s, Ha, partially

overlapped with Ha'); 1.0 [s, 12H(Ha+Ha'), $H_{a'}$]; 1.45 (s, 4H, H_f, $H_{f'}$); 1.88 (s, 2H, H_e, $H_{e'}$); 3.83 (s, 5H, H_c, $H_{b'}$, $H_{b'}$); 7.57 (s, NH). IR (cm^{-1}) 3436, 3305, 2973, 1720; 1651, 1557, 1540,

2.4.2 Synthesis of the reactive copolymer (PNIPAM/NAV/NASI)

A copolymer of N-acryloyl-N-valine, NIPAM and N-acryloxy-succinimide (NASI) was obtained by the same method as described in section 2.4.1, starting with NAV (1.704g, 10 mmol), NIPAM (2.275g,20 mmol) and NASI (101.4 mg,0.6 mmol), and AIBN (63.9 mg). At the end of the polymerization, the cooled reaction mixture was added dropwise into 500 ml of hexane to isolated the polymer. The reactive polymer was reprecipitated twice from methanol into ether, yielded 2.85 g. IR (cm^{-1}): 3432, 3151, 974, 1804, 1736, 1651, 1542, 1409, 704.

2.4.3 Pyrenyl butylamine labeled copolymer (PNIPAM/NAV/Py-an)

The reactive copolymer (2.8 g) prepared as described in section 2.4.2 was dissolved in dioxane (50 ml). Triethylamine (60 mg, 1.4 mmol) and pyrenyl butylamine hydrochloride (210.468 mg, 0.7 mmol) were added to the solution. The solution was stirred for 48 h in the dark and at room temperature, then quenched with isopropylamine (2 ml). The polymer was isolated by precipitation in ether. It was purified by two reprecipitation from methanol into ether to yield 1.8 g of pyrene-labeled copolymer(PNIPAM/NAV/Py-an). The polymer was further purified by dialysis using

dialysis tubing with the molecular weight of 12, 000. The purified polymer was isolated by freeze-dring. ^{1}H NMR (DMSO) 0.853 (s, H_a, partially overlapped with $H_{a'}$) 1.04 [s, $H_{a'}$, 12H(H_a+$H_{a'}$)]; 1.42 (s, 4H, H_f, $H_{f'}$); 1.98 (s, 2H H_e, $H_{e'}$) 3.85 (s, 5H, H_c, H_b, $H_{b'}$); 7.24 (s, NH). IR (cm^{-1}) 3436 (NH), 3305, 2973, 1715(C=O acid), 1645 (C=O amido), 1542 (NH amido), 1459, 845. UV (methanol) λ: 234, 242, 264, 276, 312, 326, 342 nm.

2.4.4 Pyrene labeled copolymer (PNIPAM/NAV/Py-ad)

Compound 5 (65.6 mg) prepared as described in 2.3.2.2, NAV (0.568 g), and NIPAM (0.758 mg) were dissolved 20 ml of dioxane. AIBN (21.35 mg) was injected into preheated, degassed solution and refluxed at 70 °C for 20 h. The polymer was precipitated into ether. It was purified by two reprecipitation from methanol into ether, yielded 0.2 g. Further purification was performed by dialysis for 10 days. The polymer was isolated by freeze-dring. ^{1}H NMR (DMSO): 0.92 (s, H_a, partially overlapped with $H_{a'}$) 1.05 [s, $H_{a'}$, 12H(H_a+$H_{a'}$)]; 1.49 (s, 4H, H_f, $H_{f'}$); 2.07 (s, 2H H_e, $H_{e'}$) 3.85 (s, 5H, H_c, H_b, $H_{b'}$); 7.37 (s, NH). UV (methanol) λ 234, 242, 266, 276, 312, 326, 342 nm.

2.5 LCST measurement

The LCST value of the polymers were determined by spectrophotometric detection of the changes in turbidity of solution heated with the constant rate of 0.4°C/min in a magnetically stirred UV cell in the temperature range of 22 to 50 °C. The turbidity of the solution was monitored at 500 nm.

2.6 Polymer molecular weight

The molecular weights of the unlabelled copolymers were evaluated from GPC. The eluent was 0.1 N NaNO$_3$ aqueous solution and PEO standards were used for calibration. The elution rate was 0.7 ml/min, the column temperature was set at a 30.0($\pm$0.1)°C. Molecular weight were estimated as those of PEO of equivalent elution volume. Mark-Houwink-Sakurada coefficients was used PNIPAM's at 30°C (K=14.5$\times$10^{-2}, α =0.5).[50a] Several batch samples were given same range of molecular weight. Since our GPC column could not set lower than 30°C at present (above the LCST of the polymers), the labeled polymer molecular weights were tried to measure by viscosity measurement.

There were no difficulty in measuring intrinsic viscosity of unlabeled polymer. The polymer was dissolving in 0.1 N NaCl aqueous at the concentrations changing from 0.5 g/l to 0.2 g/l. However, labeled polymers was shown that the flow time of polymer was smaller than that of 0.1 N NaCl. aqueous solvent It shows that the surfactant property to low the viscosity of water.

2.7 Composition of copolymer determination by acid-base titration

The compositions of copolymer were determined by acid-base titration. Potentiometric titration was carried out by measuring the pH of a solution of a copolymer as a function of the acid added volume. For each experiment , the plastic cell, thermostat set to the desired temperature 25°C, was filled 25 ml of 0.01 N NaCl in which a weighed

amount of solid copolymer (10-30 mg, dependent polymer solubility) and a known amount of standard sodium hydroxide solution. The solution was stirred magnetically, a presatured nitrogen stream (a air stream passed through a $Ca(OH)_2$ column and a water bottle, bubbled onto sample solution surface) was maintained on solution surface to avoid carbon dioxide contamination. The end point of the titration was determined at the inflection point of the pH curve to calculate the excess of sodium hydroxide equivalents. The difference between the blank amount and the equivalent of the hydroxide ions was attributed by carboxylic proton equivalent of the copolymer.

2.8 Pyrene contents determination by UV absorbance

[4-(1-pyrenyl)butyl]amine hydrochloride was used as a model compound $\epsilon=36,600$ at 342 nm in methanol solution. Absorbance of polymers in dilute methanol solution (ca 10^{-4} g/l) was measured at 342 nm.

2.9 Light Scattering

The approximate hydrodynamic diameter was obtained at 0.05 g/l of polymer in pH value of 2.5 and 9 buffer. The temperature was set at 23°C. The samples were filtered with 0.45 micrometer fresh filters several times.

2.10 Glass Transition Temperature (Tg°C)

In the heating scan (7 °C/min), the trace shows a broad endothermic peak, which

is attributed to water presented in the polymer. It is hard to see Tg due to the coverage of the broad peak. However, after samples were cooled down, reheated and very typical glass transition curve was obtained. Tg value was determined from the trace obtained in the second heating scan.

2.11 Fluorescence measurement

2.11.1 Preparation of samples

The polymers were dissolved in water and kept at room temperature for 24 h to equilibrate as stock solutions (0.45-0.5 g/l). These were further diluted into buffer or water to the desired concentration. NaI and FeCl$_3$ solutions were prepared immediatly before use. Nitromethane was distilled under vacuum before use, cetylpyridinium chloride (CPC) was recrystallized from methanol.

2.11.2 Fluorescence measurement

Fluorescence spectra were measured for 0.05 g/l of polymer solution and 25 °C unless stated otherwise. Both the excitation and emission slit widths were set at 1.5 mm. Excitation spectra were recorded with emission wavelength of 391(monomer emission wavelength) and 486 (excimer emission wavelength) nm. The scan range was 250 to 360 nm. Emission spectra were recorded with excitation wavelength of 344nm (wavelength of pyrene maximum absorbance) for PNIPAM/NAV/Py-an, or 346 nm for PNIPAM/NAV/Py-ad for samples dissolved in water or buffer. The excitation

wavelength at 342 nm for solutions in methanol. The scanning range was 360 to 600 nm. Excitation spectra were measured in ratio mode, while emission spectra were not corrected.

Quantum yield was measured for 0.05g/l polymers in water at 25°C, calculated by the following formula. Quinine sulfate monohydrate (dissolved in 0.1 N H_2SO_4 solution) was used as the standard (Φ=0.546).

$$\Phi_{unk}= \Phi_{std.} (F_{unk.}\, n_{unk}^2\, A_{std.}/)(F_{std.}\, n_{std.}^2\, A_{unk})^{50b}$$

Where Φ is the quantum yield, F is fluorescence intensity by area, n is refractive index of the solvent, and A is UV absorption of correspounding soultion. Fluorescence intensity was corrected by using "mcorr.spt" file. The excimer emission intensity (by integration area) was obtained by subtracting monomer emission from total fluorescence emission intensity. The sample monomer emission intensity (by integration area) was determined by multiplying a ratio with the monomer emission intensity (by integration area) of dilute polymer solution (no excimer emission observed). The ratio was obtained by monomer emission intensity (I_{377}) of the measured polymer solution divided the monomer emission intensity (I_{377}) of the diluted polymer solution (2.5 $\times 10^{-4}$ g/l).

3.0 Result and Discussion

3.1 Synthesis and characterization of monomers.

The monomer *N*-acryloyl-*L*-valine (NAV) was synthesized by a condensation reaction of acryloyl chloride and amino acid, *L*-valine, in sodium hydroxide solution.[2] The reaction product was obtained as a crystalline material which is soluble in many solvents, such as water, dioxane and DMSO. The structure of the product was ascertained by ^{1}H NMR and IR spectroscopy. The ^{1}H NMR spectrum of the compound exhibits a 6-proton signal at 0.89 ppm attributed to the methyl groups from valine and signals between 5.75 and 6.46 ppm attributed to the olefinic protons, H_e, H_f, $H_{f'}$. The IR spectrum presents bands at 1730, 1653 and 1620 cm^{-1} attributed to the stretching of the carboxyl, amide and carbon double bonds, respectively. The bands at 1230 and 986 cm^{-1} correspond to the OH bend of the COOH group and CH_2 bend of the carbon-carbon double bond,[50c] respectively.

The synthesis of N-[4-(1-pyrenyl)butylamine] hydrochloride (compound 4) was performed according to the procedure (Scheme 3b) reported by Winnik [37] *et al*. Pyrenyl butyric acid was converted to the acid chloride, treated with ammonium hydroxide to yield the amide which was reduced to the amine. In the ^{1}H NMR spectrum the signal of the methylene group next to the carboxyl group was shifted upfield from 2.54 (compound 1) to 1.79 ppm (compound 4) after reduction. A new 2-proton signal at 3.24 ppm attributed to C_1 methylene group of compound 4 appeared. In addition, the

structural changes due to reduction were also observed in the IR spectra. The conversion of the carbonyl group to a CH_2 group (compound 4) was evidenced by the disappearance of the carbonyl stretching band of carboxyl acid at 1694 cm^{-1}. The band at 840 cm^{-1} is attributed to polyaromatic ring C-H out of plane bending.

N-[4-(1-pyrenyl)butyl]acryloylamide (compound 5) was prepared by a condensation reaction of compound 4 and acryloyl chloride in a triethylamine methylene chloride solution. The crude product was isolated and purified by column chromatography over silica gel. In the ^{1}H NMR spectrum signals between 5.8 and 6.33 ppm are attributed to olefinic protons, and signals at 8.01 ppm to aromatic proton on the pyrene ring. The IR spectrum exhibited bands due to the stretching (1620 cm^{-1}) and CH_2 bending (977) of the carbon-carbon double bond, the amido band I (1665 cm^{-1}), the amido band II (1547 cm^{-1}) and the band at 840 cm^{-1} due to polyaromatic ring C-H out of plane bending. The UV spectrum of compound 5 presented a maximum absorption peak at 342 nm in methanol solution and its molar extinction coefficient was 36 600.

3.2 Synthesis and Characterization of Polymers:

3.2.1 Unlabeled Copolymers

3.2.1.1 PNIPAM/NAV

The free radical polymerization can be performed either in dioxane or in water solution. In order to select the best conditions for polymerization, a series of unlabeled polymers were prepared first by varying the solvent and initiator, such as dioxane, water,

and mixtures of the two (Table 2). The characterization of the products was done by ^{1}H

NMR, IR, GPC and titration (Table 2). The results indicated that both solvents were

acceptable for preparing the copolymer. Dioxane was finally selected on the basis of its

good solvent toward compound 5, its low chain-transfer efficiency and its inertness

toward *N*-(acryloxy)succinimide. All the monomers were N-alkylacrylamides, and hence

they were expected to have similar reactivity ratios. When the polymerizations are

carried out under these conditions, the copolymers precipitate during the reaction to yield

high molecular weight polymers, as shown by GPC measurements.[29]

The unlabeled polymers were characterized by ^{1}H NMR, IR, GPC and titration,

the results are listed in table 2.

Table 2: Properties of the Unlabeled Copolymers

Copolymers	Solvent/Initiator	measured monomer ratio (wt%)	feed monomer ratio (wt%)	Mw* 10^4 (Dalton)	LCST (°C)
PNIPAM/NAV (P12)	Dioxane/AIBN	36	43	2.0*	32.5
PNIPAM/NAV (P13)	H$_2$O/K$_2$S$_2$O$_8$/ Na$_2$S$_2$O$_5$	40	43	2.2	34
PNIPAM/NAV (P14)	Dioxane/AIBN	36	43	2.0	32.5
PNIPAM/NAV (P18)	Dioxane/H$_2$O(1:1, v/v) / AIBN	37	43	0.378 dl/g**	33

*measured by GPC
**intrinsic viscosity measured in 0.1 N NaCl.

The molecular weights of the copolymers were determined either by GPC or viscosity measurement. The results are listed in table 2. The following Mark-Houwink-Sakurada coefficients are used at 30 °C (K=14.5×10^{-2}, α =0.5)[48]. The several batches of samples gave all copolymers molecular weight of approximately 20,000 Dalton.

3.2.1.2 Reactive Copolymer (PNIPAM/NAV/NASI)

PNIPAM/NAV/NASI was prepared by free radical polymerization from the respective monomers (PNIPAM:NAV =2:1, molar ratio. NASI was 2% molar of the total momomers] in dioxane solution. The product was isolated by precipitation from methanol into dry diethyl ether. The presence of the *N*-hydroxysuccinimide group was ascertained from IR. The IR spectrum showed a band at 1804 cm^{-1} attributed to the carbonyl group of the lactan. *N*-hydroxysuccinimide group was not observed in ^{1}H NMR.

3.2.2 Labeled Copolymers

The labeled polymers were prepared by two procedures,[36, 37] and starting with identical ratio of monomers (scheme 4).

3.2.2.1 Copolymerization of Pyrenebutylacryloylamide, NIPAM and NAV (PNIPAM/NAV/Py-ad)

PNIPAM/NAV/Py-ad was prepared by copolymerization of NIPAM, NAV and

compound 5 in dioxane solution. The copolymer was isolated by precipitation from methanol into anhydrous ether. Further purification was performed by dialysis of the copolymer solution for 10 days, using a membrane with molecular weight cutoff value of 12,000 Dalton. The white flaky polymer was isolated by lyophilization. The structure of the polymer was determined by ^{1}H NMR, IR and UV. The ^{1}H NMR spectrum of the polymer presents signals at 0.92 and 1.05 ppm attributed to methyl groups on NIPAM and NAV, respectively. They are partially overlapping, and the total integration exhibits 12 protons. No signals were observed in the olefinic proton resonance region. Broad signals at 1.49 and 2.07 ppm are attributed to the protons of polymer backbone (CH$_2$CH). There is no signals were observed from protons of pyrene group due to the low sensitivity of the instrument. The IR spectrum shows a band at 3115 cm^{-1} due to the NH stretching of the amide, bands at 1715, 1653 cm^{-1} attributed to the carbonyl group of the COOH and the carbonyl group of the amide, respectively. A band at 1230 cm^{-1} is attributed to the OH bending of the COOH group. The bands at 1620 and 986 cm^{-1} due to the stretching and bending of olefinic group in the monomer were disappeared. The most characteristic band of the aromatic ring attributed to C-H out of the plane bending could be detected at 843 cm^{-1}, indicating successful incorporation of pyrene groups. The UV spectrum presents the typical absorption of the pyrene chromophore with a maximum band at 342 nm in methanol solution. The pyrene content was calculated to be 1.72 $\times 10^{-4}$ mol per gram of polymer or 1 pyrene per 44 monomer units (NIPAM:NAV=2:1, mol/mol), as determined by UV using compound 4 as model. The

35

COOH content of the copolymer is determined by the potential titration.[51a] The table 2 shows that the measured content of carboxylic acid is very close to that corresponding to the monomer feed ratio. In the following discussion the polymer compositions corresponding to the monomer initial feed ratio is used, namely 2: 1 of NIPAM: NAV (mol/mol).

3.2.2.2 Post-modification of PNIPAM/NAV/NASI Copolymer with 4-(1-pyrenyl)butylamine hydrochloride (PNIPAM/NAV/Py-an)

PNIPAM/NAV/Py-an was prepared by coupling compound 4 to the reactive copolymer in the presence of 2-fold molar excess of triethylamine, relative to compound 4. The reaction was conducted in the dark and monitored by TLC to detect unreacted pyrene. At the end of the reaction , the unreacted NASI groups were converted to isopropylamide by treatment with isopropylamine. The product was isolated by precipitation from methanol into dry diethyl ether. Further purification was performed by dialysis of an aqueous solution of the copolymer for 10 days, filtered prior to dialysis in order to remove any water-insoluble materials. The polymer was recovered by lyophilization. The ^{1}H NMR spectrum of PNIPAM/NAV/Py-an exhibits signals at 0.853 and 1.04 ppm attributed to the methyl groups of NIPAM and NAV, respectively. They partially overlapped and the total integration corresponds to 12 protons. No signals were detected in the olefinic proton region of spectrum. Broad signals at 1.42 and 1.98 ppm are attributed to methylene and methyline protons of the polymer backbone

(CH$_2$CH). There was no signals observed for the pyrene protons due to low sensitivity of the instrument or lower concentration of these protons. The IR spectrum of PNIPAM/NAV/Py-an shows bands at 1715, 1653 cm^{-1} attributed to the stretching of the carbonyl group of the COOH and the carbonyl group of the amide, respectively, and a NH stretching of the amido band (1542 cm^{-1}). A band at 1230 cm^{-1} is attributed to the OH bending of the COOH group. The most characteristic band of the pyrene aromatic ring at 843 cm^{-1}, attributed to C-H out of the plane bending, is observed, indicating the successful coupling of pyrenyl group to the polymer. The UV spectrum of PNIPAM/NAV/Py-an dissolved in methanol presents a maximum band at 342 nm and the characteristic pyrene absorption.. The level of pyrene incorporation was determined to be 1.50×10^{-4} mol per gram of polymer, or 1 pyrene per 50 monomer units (NIPAM: NAV=2:1 mol/mol) by UV, using model compound 4.

The molecular weight of labeled copolymer was unable to be measured by GPC and viscosity. Since we were unable to set GPC column temperature lower than 30 °C at that time (lower than the LCST of labeled polymer). On the other hand, the labeled polymer was shown that the flow time of polymer solution (concentration between 0.5-0.1g/l) was smaller than that of 0.1 M NaCl aqueous solvent in the viscosity measurement, presenting a surfactant property to lower the viscosity of water. Therefore, we assumed the labeled polymer molecular weight to be in the same range as that of the unlabeled polymer, since the molecular weight of the unlabeled copolymers was determined by GPC and are listed in table 2. Several batch samples gave the same

molecular weight range of approximatelyly 20,000 Dalton.

The carboxylic group content of the copolymer was determined by potential titration.[51:] The values are listed in table 3.

Table 3 Properties of Labeled Polymer

Polymers	PNIPAM/NAV/Py-ad	PNIPAM/NAV/Py-an
carboxyl groups content* (found, %,w/w)	39	37
λ max,** nm	342	342
Pyrene contents (mol/g. of poly.)	1.72×10^{-4}	1.50×10^{-4}
# of monomer per pyrene	44 (NIPAM:NAV=2:1)	50 (NIPAM:NAV=2:1)

* measured by titration
** measured in methanol solution.

3.3 DSC measurement:

The DSC traces exhibit a single Glass Transition Temperature Tg (table 4) and no definite melting point. Some residual bound water was present in all samples, as evidenced by the appearance of a broad transition band in the range of 55 and 180 °C in the first DSC run.[52] The Tg of PNIPAM/NAV/Py-ad determined from the second DSC run is 17 °C higher than that of PNIPAM/NAV/Py-an (table 3). This may indicate the presence of large blocks of pyrene chromophore existing in the former. These blocks are expected to possess a higher steric hindrance of the segments. In terms of the free volume model, the larger the substituents, the lower the probability of

the void volume existing, which is required to enable a thermal activated jump of the corresponding segment. Therefore, larger substituent on the polymer backbone stiffen the chain and shift the glass transition to higher temperatures.[52]

Table 4 Glass Transition Temperature (Tg, $^\circ$ C)

Polymers	Tg ($^\circ$ C)
PNIPAM/NAV (P12)	125
PNIPAM/NAV/Py-ad	141
PNIPAM/NAV/Py-an	123
*PNIPAM	85 /103 [53]/ or 130 [54]

*literature reported

3.4 Solution Properties of the Polymers

3.4.1 Lower Critical Solution Temperature (LCST)

The polymers were soluble in water at or below room temperature. The pH of the copolymer solution was 4.1 for a polymer concentration of 2.5 g/l. As expected, the aqueous solutions became turbid when heated, indicating the occurrence of a lower critical solution temperature (LCST). The LCST of the polymers are listed in table 5. The LCSTs of the unlabeled polymers in water(32.5 -34.0 °C) are slightly higher than that of PNIPAM (32.0 °C).[55-57] The LCST of the labeled polymer, PNIPAM/NAV/Py-ad in water (32.5°C), was identical to that of PNIPAM/NAV, but the LCST of

39

PNIPAM/NAV/Py-an in water (28.5 ° C) was lower than that of PNIPAM/NAV. It is well known that changing the hydrophilic/hydrophobic balance causes a change in the LCST. The copolymers studied here contain the pyrenebutyl amide groups which are the hydrophobic and *N*-acryloyl-L-valine which are the hydrophilic. It can be seen (table 4) that the attachment of hydrophobic pyrene on the PNIPAM/NAV/Py-an backbone has a significant effect on the phase transition process in the case of PNIPAM/NAV/Py-an, which has an LCST 4 °C lower than PNIPAM. In contrast, the attachment of the hydrophobic pyrene on the PNIPAM/NAV/Py-ad backbone did not have a significant effect on its LCST. A similar phenomenon was reported in hydrophobic modified PNIPAM such as b-PNIPAM-$(C_{18})_2$ /280,[56] which suggested that in one case the hydrophobic substitutents are not exposed to water, but rather form a micellar structures protected from water by the NIPAM and NAV chain. Therefore, this does not make a hydrophobic contribution to its LCST.

3. 4 .2 pH effect on LCST

The LCST of the copolymers in aqueous solutions of various pH value are presented in the table 4. The LCST of PNIPAM/NAV at pH value of 4 is lower than that of PNIPAM, the LCST of the labeled copolymers are even lower (24 °C for PNIPAM/NAV/Py-ad, 25.5 °C for PNIPAM/NAV/Py-an). It is known that the LCST is caused by a critical balance between hydrophobic and hydrophilic domains in the polymer side groups that trigger the formation of a layer of a highly organized water molecules around the macromolecular chains. As temperature increases, hydrophobic

interactions are enhanced by the weakening of hydrogen bonds between water molecules and amide groups of the polymer. The presence of charged groups shows that electrostatic and hydrophobic forces compete. The ionization of the carboxylic groups in the copolymer chains will give rise to electrostatic repulsion along the chain and result in the expansion of the originally coiled molecule. The protonated form of the polymer should be assumed to be a compact coil conformation where short-range attractive interactions outweigh electrostatic forces. Hydrophobic groups on the polymers may provide a further chain contraction, and in some cases the polymer precipitates because the hydrophobic moieties overcome the hydrophilic quality of the carboxyl groups at a relative low charge density. Our observations can be interpreted in terms of the complex formation by the efficient formation of hydrogen bonds between the amide groups of NIPAM units and the protonated carboxylic groups of NAV at a low pH value. The hydrogen bonding prevents the access of water molecules to the amido groups, thus rending the polymer chain more hydrophobic, so as to decrease their phase-separation temperature.[9]

At high pH (≥ 9), the -COOH groups are completely ionized and the hydrogen bonds between the amido and the carboxyl groups are disrupted, which dramatically increases the hydration of the polymers, i.e. more hydrogen bonds are formed between water and either the amido or the carboxyl groups. The repulsive forces between the negative charges on the polymer are much larger than the attractive forces between hydrophobic moieties. Therefore, the polymers aggregate only at a relatively higher

41

temperatures or even remain soluble over the entire temperature range.[30] A similar

phenomenon was also reported by Hoffman et al. [30, 59, 60]

Table 5 LCST of Copolymers

pH**** (±0.01)	LCST (°C)		
	PNIPAM/NAV**	PNIPAM/NAV/Py-an***	PNIPAM/NAV/Py-ad***
4.00	28.7	25.5	24
7.00	28.7	26.5	26
9.00	34.5	Not observed	Not observed
12.10	38.5	Not observed	Not observed
Water*	32.5	28.5	32.5

*   pH of polmers in water: 4.1
**   polymer concentration 2.5 g/l
*** polymer concentration 0.43 g/l
**** pH buffer

3.4.3 Light Scattering.

The formation of polymers aggregates/ or micelles in water was confirmed by

light scattering experiments. Large aggregates were detected in buffered solutions of the

copolymer (0.05 g/l) at 23 °C. The effective diameters of the polymeric aggregates are
listed in table 6.

Table 6 The Effective Diameter of the Copolymers in Buffer

Polymer	Effective Diameter (nm)	Polydispersity	I_E/I_M
pH=2.50			
PNIPAM/NAV/Py-ad	292	0. 11+0.08	0.365
PNIPAM/NAV/Py-an	327	0.13+0.05	0.137
PNIPAM/NAV	243	0.14+0.05	
pH=9.00			
PNIPAM/NAV/Py-ad	58	0.13+0.06	0.661
PNIPAM/NAV/Py-an	40	0.19+0.06	0.155
PNIPAM/NAV	55	0.29+0.09	

Micelles formed by simple amphiphiles are usually quite small, with an
aggregation number of the order of 100. Their formation clearly requires the existence of
two opposing forces, attractive force favoring aggregation and a repulsive force that
prevents growth of the aggregates to large size. Even in systems where much larger

micelles are formed a repulsion force must be present, to prevent separation of the amphiphile into an entirely distinct phase. For micelles in aqueous solution, the attractive force arises from the hydrophobic effect acting upon the hydrocarbon chains (exhibited by the alkyl-pyrenyl groups and isopropyl groups) of the amphiphile. The repulsive force in micelle formation must come primarily from the head groups. In ionic micelles the electrostatic repulsion between deprotonated carboxylic groups is a major factor. In micelles formed by amphiphiles with the protonated carboxylic head groups, excluded volume repulsion between the polymers opposed to self-association. The balance of these two forces is expected to depend not only on the molecular architecture of the copolymers but also on the application of external stimuli, such as changes in pH values. Table 6 shows that aggregates are larger in acidic conditions compared to the basic conditions, however, in basic condition the micelles sizes of copolymers are comparable to those (38-72 nm) of hydrophobically modified PNIPAMs [56], indicating that there is a much stronger intermolecular attractive interaction at a pH value of 2.5 than pH value of 9. This fact suggests that stronger attractive interactions are contributed by hydrophobic interaction and complex formation in acidic conditions[61-63]. From the calculated polydispersity values it is apparent that there is a broad distribution of micelles sizes.

3.5 Fluorescence Properties

3.5.1. PNIPAM/NAV/Py-ad

The emission and excitation spectra of solutions of PNIPAM/NAV/Py-ad in both water and in methanol were measured at 24 °C. In the fluorescence spectrum (figure 1), the polymer in methanol solution shows an emission due to the locally excited pyrene chromophores (I_M, Intensity of monomer emission) with the [0, 0] band located at 377 nm and a broad emission centered at 481 nm due to pyrene excimer emission (intensity I_E). The relative ratio of emission intensities of excimer (I_E) at 481 nm and monomer (I_M) at 377 nm can be used to elucidate the behavior of polymer in solution. When the polymer is dissolved in a good solvent such as methanol, the polymer coil is consequently expanded, a small I_E/I_M value of 0.39 of PNIPAM/NAV/Py-ad was obtained. The excitation spectra monitored for the monomer (391 nm)and the excimer (481 nm) were identical (figure 2a). The maxima correspond to those in the UV absorption spectrum.

Solutions of the copolymer in water exhibit a strong excimer emission centered at 486 nm the ratio I_E/I_M 0.72 (taken 377 nm band as I_M) is larger than that obtained from a methanol solution ($I_E/I_M=0.39$) (figure 1), suggesting that there is a much stronger aggregation in water than in methanol. The excitation spectra (Figure 2b) in water monitored for monomer and excimer are different. The general features are similar, but the former is blue-shifted ($<\lambda$: the difference in wavelength maxima for the (0,0) transition in the excitation spectra viewed at the excimer emission and the monomer emission) by 2.5 nm. The bands monitored for the excimer are broadened, the peak-to-valley ratio in the excitation spectrum viewed at monomer, P_M and excimer, P_E are relative measures for this broadening (table 5). In a situation where pyrene preassociation

45

takes place P_E is always smaller than P_M. Comparison with the UV spectrum of an aqueous solution of the polymers reveals that it is the excitation spectra for excimer that corresponded to the UV absorption. The UV spectrum of the polymer in water has a maximum absorption band at 346 nm, compared to 341 nm for solution in methanol. They exhibit a strong hypochromic effect (preassociation of the chromophores results in a broadening of the absorption bands and a red-shift of the maximum position).[64] The extinction coefficient for the pyrene chromophore at 346 nm decreased from a value of 36,600 in methanol at 342 nm band to 19,000 in water. All these observations lead to the conclusion that in aqueous polymer solution, the excimer originates from pairs of aggregates of pyrenes that exist prior to excitation. This phenomenon has been observed in other polymers such as pyrene-labeled PNIPAM.[37,38]

Table 7 Photophysical Parameters of PNIPAM/NAV/Py-ad

and PNIPAM/NAV/Py-an in Solution*

parameter	PNIPAM/NAV/Py-ad		PNIPAM/NAV/Py-an	
	Water	Methanol	Water	Methanol
I_E/I_M	0.72	0.39	0.15	0.14
λ_E, nm	486	481	486	480
P_M	1.094	2.011	2.06	2.438
P_E	1.539	1.984	1.62	2.368
$\Delta\lambda$, nm	2.5		2.5	
P_A**	1.35	2.187	2.34	2.6487
Φ_M	0.117		0.259	
Φ_E	0.108		0.018	
Φ_t	0.225		0.277	

* Polymer concentration: 0.05g/l
** Peak to valley ratio for the (0, 0) transition in absorption

The ratio of I_E/I_M was measured as a function of polymer concentration in order to determine whether pyrene ground state aggregates form between chromophores attached to the same polymer chain or between chromophores from different polymers. The values I_E/I_M were determined for polymer solution over as a wide concentration

range as possible. This range was limited on the dilute end to 10^{-5} g/l, by the inability to measure reliable fluorescence intensities. The high concentration was limited to 0.5 g/l, by insolubility of the polymer in water. The ratio of I_E/I_M remained constant over the polymer concentration range of 10^{-5} to 10^{-3} g/l , then it increased abruptly as the concentration increased (figure 3). The inflection point appeared at 0.01 g/l, which was taken as the critical aggregation concentration of the polymer (CAC).[62, 65] This result indicates that only intrapolymeric interaction occur at low concentration, when the polymer concentration is higher than about 0.01 g/l both inter- and intra-polymeric interactions occur. The formation of such micellar structures in aqueous solutions of PNIPAM/NAV/Py-ad was confirmed by light scattering as mentioned earlier.

Temperature Effects

Figure 5 presents the ratio I_E/I_M of PNIPAM/NAV/Py-ad aqueous solutions as a function of temperature. When the temperature of the polymer solution was increased from 15 to 60 ° C, the ratio of I_E/I_M increased slowly until it reached a maximum value of 0.75 at 30° C, then decreased sharply to a limiting value of 0.303 at 55 °C. It is interesting to note that, unlike PNIPAM [5], the monomer emission of PNIPAM/NAV/Py-ad decreased only slightly when temperature increased, but the excimer emission dramatically decreased while the temperature increased above the LCST. This result may indicate that non-emitting chromophore aggregates are disrupted near and above the LCST of the polymer solution. The chromophore was isolated from each other to its

maximum extent. A blue-shift of excimer emission was observed from 486 nm at 20° C to 478 nm at 60 °C (figure 5).

pH Effect on Fluorescence

Figure 6 shows the changes in I_E/I_M of PNIPAM/NAV/Py-ad aqueous solutions as a function of pH. As discussed previously (section 3.5.2), the polyelectrolyte chains adopt an extended conformation at high pH values due to electrostatic repulsion between the negatively charged carboxylic groups on the polymer chain. As the pH decreases the polymer contracts to a coiled conformation. This transition is expected to lead to an increase in I_E/I_M[66-68]. Therefore one would expect a lower value of I_E/I_M at high pH, compared to solution of low pH. However, we observed that I_E/I_M of copolymer PNIPAM/NAV/Py-ad increases with increasing pH from 2.5 to 12.1, namely from 0.192 to 0.619 for a polymer concentration of 0.025 g/l while the pH value changed. Since the carboxylic acid groups function as proton-donating moieties and amide groups as proton-accepting moieties could associate by hydrogen bonding. The association (complexation) is strongly dependent on pH of the system (diagram 4). The existence of a certain number of protonated carboxylic groups is necessary to form a stable complex through hydrogen bonding. At relatively low pH values the number of protonated COOH groups is very high and a large number of hydrogen bonds can form between polymer chains. A large number of hydrogen bonds and a small separation between hydrogen-bound groups would result in a strong complexation and would also

constrain any segmental mobility. This situation is similar to network cross-linking which limits segmental movement. Therefore, the associated chains are very stiff, resulting in a low value of I_E/I_M. With increase in the pH, some of the acidic groups deprotonate, resulting in break up the hydrogen bonds. Thus, the distance between some hydrogen-bound groups increases and the segmental mobility of associated chain also increases. The measured I_E/I_M should increase, as was observed in figure 6. Finally, at a pH value of 7, almost all the acid groups are deprotonated, and the segmental mobility became large enough to overcome the strength of hydrogen bonds, breaking the complexes apart. [49, 69, 70] Thus, it is expected that the excimer intensity increases in basic conditions (diagram5).

The ratio of I_E/I_M underwent only a small increase with increasing pH in solution higher concentration (0.05 g/l) compared to the diluted solution (figure 6a.). The smaller change of I_E/I_M may be attributed to the formation of a network structure since the compact polymer chains tend to interpenetrate in high concentrations. The excimer emission underwent blue-shift with decreasing pH values (figure 7). A blue shift of 6 nm was observed at pH value of 2.5 and polymer concentration of 0.025 g/l. This result indicated that the copolymer aggregated forming a more microhydrophobic domain in acidic conditions than basic conditions due to release some bounding water molecules from the polymer chains. This further supports the idea that the complex was formed at a low pH value. A similar phenomena were reported by P. Somasundaran and his coworkers.[40-42]

3.6. 2 PNIPAM/NAV/Py-an

The emission and excitation spectra of PNIPAM/NAV/Py-an solution in water and in methanol were measured at 24 °C (figure 8). Methanol solution of the polymer exhibites that the fluorescence spectrum is dominated by a strong monomer emission (I_M) at 377 nm. Only a small broad excimer emission centered at 480 nm (I_E) was detected (I_E/I_M 0.14) (table 7). The excitation spectra monitored for monomer (391 nm) and excimer (480 nm)coincide (figure 9). The P_E value(2.37) is slightly smaller than the P_M value (2.44). The maxima correspond to those in the UV absorption spectrum. The spectrum of PNIPAM/NAV/Py-an in ater also presents a strong monomer emission and a small broad excimer emission centered at 486 nm. The I_E/I_M (0.15) was almost the same value as that in methanol. This suggested that the pyrene groups are distributed homogeneously. The excitation spectra in water monitored for monomer (391 nm) and excimer (486 nm) do not coincide, but have a blue-shift about 2 nm. Its P_E (1.62) is smaller than P_M (2.06, table 6). The UV spectrum of PNIPAM/NAV/Py-an in water has a maximum band at 344 nm, compared to 340 nm in methanol. It also exhibits a strong hypochromic effect accompanied by bands broadening and decrease the extinction coefficients.

The ratios of I_E/I_M were measured as a function of polymer concentration.The results were similar to those observed with PNIPAM/NAV/Py-ad. The ratio of I_E/I_M remained constant over the polymer concentration range of 10^{-5} to 10^{-3} g/l, then it increased abruptly with increasing of polymer concentration (figure 10). The inflection

point observed was about 0.01 g/l, which was taken a critical aggregation concentration of the polymer (CAC). [62, 65] This result indicates that only intrapolymeric interactions form in relatively low polymer concentration and that there are both inter- and intra-polymeric interactions coexisting when the polymer concentration is higher than about 0.01 g/l.

The individual quantum efficiencies of the monomer and excimer emission and the total quantum yields of emission (Φ_T) are listed in the table 6. The total quantum yields of pyrene emission are nearly same for both polymer. However, the excimer quantum yield of PNIPAM/NAV/Py-ad (0.108) is much higher than that of PNIPAM/NAV/Py-an (0.018), which is in an agreement with the fluorescence result.

pH effect on fluorescence

As noted in the case of PNIPAM/NAV/Py-ad, the I_E/I_M of PNIPAM/NAV/Py-an is pH dependent (figure 11). At a polymer concentration of 0.05 g/l, the ratio I_E/I_M increased significantly at low pH (pH<7), reached maximum at pH 7 (approximate), then slightly decreased as pH value increased to 12. For solution of lower polymer concentration (0.005 g/l), a larger increase in I_E/I_M from 0.05 to 0.12 is observed (figure 11). The excimer emission of the polymer was blue-shifted up to 13.5 nm with decreasing pH value to 2.5 at the polymer concentration of 0.1 g/l (figure 12). This may indicate that the complex formation between the amide and the carboxylic groups of PNIPAM/NAV/Py (diagram 6). Again, these results indicates that PNIPAM/NAV/Py-an aggregates have more hydrophobic micro domains under acidic conditions than basic

conditions. This further confirmed the complex formation between the amide and the carboxylic groups at acidic conditions releasing some water molecules from the polymer chains.

It is interesting to note that PNIPAM/NAV/Py-an showed a strong monomer emission in water, PNIPAM/NAV/Py-ad showed a strong excimer emission, although fluorescence measurement as a function of the polymer concentration as well as light scattering investigations corroborated to indicate the existence of polymeric micelles in water. It seems that in the micelles of PNIPAM/NAV/Py-ad the hydrophobic groups are "protected", but the micelles of PNIPAM/NAV/Py-an do not provide such protection. This will be discussed next.

3. 5. 3 Comparison of the two polymers

The fluorescence spectra of the two labeled polymers showed dramatic differences in terms of the ratio of excimer emission to monomer emission in aqueous solution. The I_E/I_M ratio of PNIPAM/NAV/Py-ad has a value almost 5-fold larger than that of PNIPAM/NAV/Py-an (Table 6), indicating that the former polymer may possess some inherent blockiness or short runs of chromophore label. Further support to this assumption comes from the facts of that the Ie/Im ratio of PNIPAM/NAV/Py-ad in methanol solution still remained high (0.36) and much higher that the Ie/Im ratio (0.15) of PNIPAM/NAV/Py-an and that its Ie/Im even remained high (0.30) even at 60 °C in the aggregates. DSC results (see previous) are consistent PNIPAM/NAV/Py-ad

with the occurrence of blockiness chromophore substituted monomeric units. The first procedure used to prepare a more homogeneous distribution of labeled copolymer PNIPAM/NAV/Py-an. Hence, we may be able to assume that most of the micelles formed by the homogeneously distributed hydrophobically labeled polymer PNIPAM/NAV/Py-an contain isolated pyrene, but most of micelles formed by the blocky hydrophobically labeled polymer PNIPAM/NAV/Py-ad contain more than one pyrene hydrophobic group in close approximate, this can lead to the difference in their LCST value and temperature effect on fluorescence properties.

It was mentioned previously that the I_E/I_M ratio of PNIPAM/NAV/Py-an slightly changed with increasing temperatures. Aggregation of polymer chains increases with increasing temperature, however it does not give more chance to let the chromophore aggregation since only a limited pyrene number exist in most of micelles. Therefore the excimer emission of PNIPAM/NAV/Py-an does not exhibit significant change. Based on the results of PNIPAM/NAV/Py-ad and PNIPAM/NAV/Py-an, one may suggest that temperature dramatically influenced only on excimer emission of this kind of copolymers.

The first procedure not only yields a more homogenous labeled microstructure copolymer, it is also faster and consumes less pyrene probe. The overall yield of the compound 4 was 30-35% but only 8-10% for compound 5. In addition compound 4 was much easier to purify than compound 5.

\

3.6 Quenching Study

In order to further probe the microenvironment of the pyrene fluorophore, we studied the quenching of fluorescence of the labeled polymers, by a cationic quencher [Fe(aq) $^{3+}$], an anionic quencher (I^-), a surfactant quencher (cetylpyridinium chloride, CPC) and a neutral quencher (nitromethane).

Fluorescence quenching can occur through a variety of processes including excited state reactions, energy transfer, complex formation, and collision quenching.[71] Fluorescence quenching has been widely studied as a fundamental phenomenon. Quenching resulting from a collision encounter between a fluorophore and a quencher is called collision or dynamic quenching. Static quenching results from the formation of a nonfluorescent complex between fluorophore and quencher. In either case, the fluorophore and quencher must be in contact.

The close approach of fluorophore and quencher can be prevented by electrostatic repulsion. Iodide I^- is a negatively charged quencher and one can expect that it will be repelled by negative charges (COO^-) surrounding a fluorophore. Similarly the ferric Fe(aq) $^{3+}$ ion should be attracted towards a fluorophore in a negatively charged environment. Such attraction and repulsion will depend also on the ionic strength of the solvent. They are expected to decrease in solutions of increased ionic strength. In contrast to ionic quenchers, neutral quenchers like nitromethane are not expected to be sensitive to the charge surrounding a fluorophore [71] or to the ionic strength of the solvent.

In Manning's counterions condensation theory,[72-76] polyelectrolytes in aqueous

solution are characterized by a dimensionless charge density parameter ξ given by

$$\xi = e^2/ \epsilon kTb \qquad (3)$$

where e is the protonic charge, ϵ is the dielectric constant of the solvent, k is Boltzmann constant, T is the kelvin temperature, and b is the average axial spacing between charged groups on the polymer. The value of b=2.55Å [74] is ordinarily used for vinyl polymers carrying an ionic charge group on each monomeric unit.[35] Therefore the value of ξ=2.8 [74] is commonly used for a fully extended vinylic polyion in aqueous solution at room temperature. The critical charge density parameter is defined as $\xi_c = N^{-1}$ [ξ_c of Fe(aq)$^{3+}$ is 0.333], where N is the counterion valence. When $\xi > \xi_c$, the counterions are condensed until the effective charge density parameter (ξ_{eff}) equals Lc. When $\xi < \xi_c$, on the other hand, the counterions are completely dissociated.

3.6.1 Interaction with nitromethane neutral quencher

Fluorescence quenching did not change the shape of all steady-state spectra but affected their overall intensity. Figure 13 presents the nitromethane quenching of PNIPAM/NAV/Py-ad and PNIPAM/NAV/Py-an. The quenching data were plotted in terms of the Stern-Volmer equation [71] (eq. 4).

$$I_0 /I = 1 + Ksv [Q] \qquad (4)$$

where Ksv is the Stern-Volmer quenching constant, I_0 and I (taken at 377 nm band) are the emission intensity in the absence and presence of a quencher, respectively, [Q] is the quencher concentration. A linear Stern-Volmer plot is generally indicative of a single

class of fluorophores, all equally accessible to quencher. The mechanism should be either purely static or purely dynamic quenching process. The Stern-Volmer constants for monomer emission of these two copolymers quenching by nitromethane are essentially identical, they are 238 and 277 M^{-1}, respectively. The relative low Ksv suggested that the quenching mechanism would be contributed by dynamic quenching process. However, the Stern-Volmer constant for excimer emission of PNIPAM/NAV/Py-ad is only 85 M^{-1}, which is much less than that of PNIPAM/NAV/Py-an (171 M^{-1}), both of them are also less than that of monomer emission, indicating that nitromethane as the water-soluble neutral quencher has the larger efficiency to quench monomer emission than that of excimer emission. This is further suggested that pyrene monomer must locate in a more hydrophilic microenvironment than pyrene excimer, and that nitromethane interacted more strongly with PNIPAM/NAV/Py-an, which has homogenous hydrophobic pyrene label, than PNIPAM/NAV/Py-ad.

3.6.2 Interaction with cationic quencher

In this section we investigated how the polyelectrolyte influence the environment for the fluorescence quenching reaction between the pyrene chromophore bound to polyelectrolyte and charged quenchers. In th immediate vicinity of the polyelectrolyte, there exists a so-called "restricted reaction space" [RRS] [77] where one can define a RRS as a molecular level environment that directly affects the course of a reaction. This is in accordance with other work in which micelles, DNA, sol gels and biological receptor sites were also considered as RRS [78-80].

Steady-state fluorescence quenching experiments were performed in water and in a series of buffer solutions using Fe^{3+} (from $FeCl_3$) as the quencher. Fluorescence quenching was measured as a function of concentration of the quencher below and above the LCST. In the case of salt-free water medium (pH=3.90), the Stern-Volmer plot for the quenching of pyrene emission in PNIPAM/NAV/Py-an by $Fe(aq)^{3+}$ was linear for [$FeCl_3$] lower than ca. 10^{-4} M (Figure 14) with a Stern-Volmer constant of 1.72×10^{4} M^{-1} (table 8). The same experiments were performed with polymer solution of 0.05 g/l at pH value of 2.50 and 9.00, the Stern-Volmer plots for the quenching of the monomer and excimer emissions (figure 15) were also linear with Stern-Volmer constants listed in table 8. It was observed that the Stern-Volmer constant for quenching of monomer emission at pH 9 is 3-fold (358 M^{-1}) larger than that at pH 2.50 (115 M^{-1}). Moreover the quenching efficiency was much higher (over 100-fold) in neutral water than in either acidic or basic buffers. Thus, one can see that the quenching efficiency depends on pH and on the ionic strength of the system.

At low pH (2.50), the quenching process is strictly restricted. This can be explained the fact that at low pH, the completely protonated polymer chains form self-complexes and adopt a more compact and rigid conformation, which decreases the probability of pyrene probe to form a complex with $Fe(aq)^{3+}$ or restrict the accessiblility of quencher to pyrene. i.e. the formation condensed counterion is restricted due to a low concentration of free carboxylic groups.[74-76] At high pH (9.00), the carboxylic groups are completely ionized and the polymer chains are extended to the largest extent. The

negative charges in the polymer chains increase the local concentration of the cationic $Fe(aq)^{3+}$ around polymer. The charge density ξ of the deprotonated copolymer was 1.2 and average axial spacing between charged groups on the polymer was 5.93Å (calculated from equation 3).[35, 74] The ionized polymer chain made a much easier condition to form condensed counterion, therefore, the quenching rate is accelerated with increasing pH and the negative charge of polymer.[74, 81] As expected that quenching efficiency in this basic buffer should be lower than that in pure water (reduced over 100-fold).[77] This can be explained by the fact that the ionic strength is much stronger in the buffer (100 mM from added NaCl) than that in the salt-free water (ionic strength is ca. 10^{-3} mM as taken an average from quencher $FeCl_3$, and the contribution of polyanion to the ionic strength was not included)

The remarkably high reaction rate observed in pure water is a result of the equilibrium accumulation of quencher ions in the immediate vicinity of the polyion.[82] Two types of factors can contribute in this situation. The first is simply statistical, in which quencher ions are randomly replaced in this near region by the added salt (from buffer). The second is dynamical, as the diffusion dynamics will experience the decrease of electrostatic potential near the polyion with increasing salt concentration.[77] In addition, the polyanion conformation changes may play a role as will be mentioned next.

However, the observed data for both monomer and excimer emission deviate from the linear Stern-Volmer plot at relative high quencher concentration (higher than ca. 10^{-4} M, Figure 14). One may infer that the polyelectrolyte solution contains a

nonuniform distribution of quenchers and fluorophores when the quencher concentration or the ionic strength is high. The change in ionic strength could cause a structure change of polyelectrolyte such that the polymer is coiled, which may protect the pyrene chromophore inside a inner hydrophobic microenvironment, acting as a steric hindrance to pyrene.   Since the coiling of polymer is statistical, there must be some chromophores that would be protected against the quencher while another fraction of chromophore is accessible to quencher.

Downward curvature indicated two populations of fluorophores existed in this system, one is inaccessible to quencher, where the other fraction is accessible to quencher.   The accessible fraction of chromophore can be estimated by applying a modified Stern-Volmer model derived for systems in which there are heterogeneities in quencher and in chromophore concentration and diffusion coefficients.[71] This model assumes that only a fraction f_a of the fluorophore is readily quenchable, while a fraction $(1-f_a)$ is protected against quenching. The fraction of accessible chromophores and the Stern-Volmer quenching constant Ksv of this accessible fraction can be obtained from the following equation.[82]

$$I_0/I = \{ \ 1- (fa \ Ksv \ [Q]) \ / \ (1+Ksv \ [Q] \ )\} \tag{5}$$

In summary, the quenching process achieves maximum efficiency at low ionic strength.   Approximately 88.6% of pyrene monomer has been quenched while the quencher concentration was up to 5×10^{-4} M.

In order to determine the quenching mechanism, the same measurements were

done at 31 °C.[71]   The efficiency of static quenching depends on the stability of complex. Since higher temperature is likely to result in a decrease stability of complexes, we expected to observe lower values of the static quenching constants.   The efficiency of dynamic quenching depends on diffusion. Increasing temperature results in larger diffusion coefficients, so that the bimolecular quenching constants are expected to increase with increasing temperature.   The Stern-Volmer plots determined at 31 °C also presented a downward the value (figure 16). It is important to note that the Ksv values in water are high at 31 °C, compared with room temperature. This might suggest that a static mechanism takes place in this quenching system. This temperature is above the LCST of PNIPAM/NAV/Py-an. The aqueous solution of the polymer undergoes aggregation which must decrease the quenching efficiency.[82]

In case of PNIPAM/NAV/Py-ad, the Stern-Volmer plots for monomer and excimer emission quenching also showed a downward curvature within the same quencher concentration range as PNIPAM/NAV/Py-an's (figure 17). At low quencher concentration, I_0/I increased rapidly.   Only a slight increase of the ratio was observed for $FeCl_3$ concentrations higher than ca 10^{-4} M. Quenching of pyrene excimer emission was more efficient than that of the monomer. Modified Stern-Volmer equation (equ. 5) was used to draw a "theoretical" curve I (figure 17, solid line), the experimental data fit this equation. Estimated values of Ksv and f_a were listed in the table 8.

Table 8 Parameters of Polymers Quenching by FeCl$_3$

		Ksv (M^{-1}) in water (pH=3.90)		Ksv (M^{-1}) in buffer pH=9.00 PH=2.50	
		Ksv (M)*	Ksv (E)**	Ksv (M) Ksv (E)	Ksv(M) Ksv (E)
PNIPAM/ NAV/Py-an	25 °C	1.74e+4	5.30e+4	358 2.64e+3	115 3.10e+3
	31 °C	3.60e+3	8.0e+3		
PNIPAM/NAV /Py-ad (25° C)		1.02 e+4 fa=0.874	2.32e+4 fa=0.919		

* Ksv (M): Stern-Volmer constant of monomer
** Ksv (E): Stern-Volmer constant of excimer

At room temperature, according to equation 2 in the dilute PNIPAM/NAV/Py-ad solution, a fraction of 13.6% pyrene monomer of PNIPAM/NAV/Py-ad is inaccessible to quencher, hence must be located in a hydrophobic environment. One possibility that would create such microdomains is interchain association.[82] It has been shown by DSC and steady-state fluorescence measurement that polymer aggregation takes place below the LCST, this further confirms protected fraction of pyrene might be from blocky distribution of the label, i.e. the blocky pyrene of PNIPAM/NAV/Py-ad was buried in the interior of hydrophobic microdomain (diagram 7).

Surprisingly, at low quencher concentration the excimer fluorescence was quenched more efficiently than monomer fluorescence. This suggests that the trivalent

counterions have a strong tendency for a site binding and therefore are more intimately involved with polyions. The larger Ksv of PNIPAM/NAV/Py-an indicated that the quencher $Fe(aq)^{3+}$ interacted more strongly with PNIPAM/NAV/Py-an than with PNIPAM/NAV/Py-ad.

3.6.3 Interaction with an anionic quencher

Iodide I⁻ is a negatively charged quencher of pyrene fluorescence. Therefore, it is expected that it would be repelled by negative charges (COO⁻) surrounding a fluorophore, in contrast, to the cationic $Fe(aq)^{3+}$ that is attracted towards a fluorophore in a negatively charged environment. As mentioned earlier, such attraction and repulsion depend on the ionic strength of the solution. Figure 17 shows the quenching intensity of monomer and excimer versus the quencher concentration in water and in the pH value of 2.5 and 9 buffers.

In case of PNIPAM/NAV/Py-an the Stern-Volmer plot measured in water medium was linear (figure 18a), its Ksv (M) and Ksv (E) was 20 and 7 M^{-1}, respectively (table 8). The quenching efficiency of iodide in this system is extremely low, a fact attributed to the electrostatic repulsion between the two negatively charged species. A similar straight line was observed while the polymer concentration decreases 10-fold over the same quencher concentration range as quenching of 0.05g/l polymer (figure 18a).

In case of PNIPAM/NAV/Py-ad, figure 18b, the Stern-Volmer plot presented downward curvature plots in the same quencher concentration range as that of

PNIPAM/NAV/Py-an. As discussed above, this downward curvature originates from the fact that a fraction of chromophores are inaccessible to the quencher. The accessible fraction was analyzed using a modified form of Stern-Volmer equation (equ. 5). The calculated Stern-Volmer constant of quenched fraction is listed in table 8.

This downward curvature could stretch out and approach a straight line when the polymer concentration decreased 10-fold and the quencher concentration remained same range (figure 18b), providing further evidence that the downward curvature was dominated by charge repulsion in this case. The same experiments were performed in buffer solution (Figure 19). As expected the quenching efficiency (Ksv=19) in the basic buffer (pH=9.00) was lower than that (Ksv=112) in the acidic buffer (pH=2.50), which indicates the difference in the environment of pyrene between the neutralized and charged polymer resulted from the "restricted reaction space" effects that the polymer imposes on the approach of quencher I^- [83]. The quenching of excimer is essentially inefficient in water and in the basic buffer, indicating that the hydrophobic microenvironment created by the negative polymer chains inhibits the water and hydrophilic negative iodide to the pyrene excimer (diagram 8). The mechanism of interaction is more complicated in the acidic condition.

Table 9 Parameters of PNIPAM/NAV/Py-ad Quenched by NaI

	Ksv (M)	fa
water	55	0.672
pH=2.50 buffer	112	0.703
pH=9.00 buffer	19	1.0

Quenching of the accessible pyrene residues potentially allows the emission spectra of the accessible and inaccessible residues to be resolved. Upon selective quenching of pyrene by I$^-$, the remaining fluorescence resulting from the buried pyrene can be determined. And these are expected to be blue shifted relative to the quenched residues. The quenched residues are expected to be exposed in the more hydrophilic microenvironment, hence red-shifted. Figure 18a shows that the emission spectra of PNIPAM/NAV/Py-ad quenched by I$^-$ The emission spectra were blue-shifted (1-2 nm) upon quenching.

In the separation of the accessible and inaccessible fraction of the total fluorescence it should be realized that there may be more than two classes of pyrene residues. Even the presumed "inaccessible" fraction may be partially accessible to quencher.

3.6.4. Interaction with cationic surfactant quencher

In order to probe the hydrophobicity of the labeled polymer, a hydrophobic quencher, CPC, was employed as a quencher. CPC is a surfactant with a critical micelle concentration of 8×10^{-4} M.[39] Its pyridinium ring is an oxidative quencher. Figure 20 shows the monomer and excimer intensity quenching curves of the copolymers by CPC in water. In the case of PNIPAM/NAV/Py-ad, a linear Stern-Volmer plot was obtained for both monomer and excimer emissions, with constants were 1.57×10^{4} and 2.25×10^{5} M, respectively. Again, the linear Stern-Volmer plot indicates either pure static or dynamic process. The large Ksv suggested that its mechanism might be contributed by static quenching.

Table 10 Polymers Quenching Parameters in Water

| | PNIPAM/NAV/Py-ad | | PNIPAM/NAV/Py-an | |
	Ksv(M)	Ksv(E)***	Ksv(M)	Ksv(E)
nitromethane	238	85	277	171
CPC	1.57e+4 5.0e+4**	2.25e+5 2.44e+5**	2.08e+4 *	1.85e+5*
FeCl3	1.02e+4 fa=0.874	2.32e+4 fa=0.919	1.72e+4	5.30e+4
NaI	55 fa=0.672	0	20 22.2**	7.0 1**

* initial slope of upward curvature.
** polymer concentration 0.005g/l
*** Ksv unit: M^{-1}

In the case of PNIPAM/NAV/Py-an theStern-Volmer plots quenching by CPC (figure 23) showed upward curvature, indicating that quenching includes both static and dynamic quenching processes. The high initial slope (2.08e+4 M^{-1}) must be a consequence of predominantly static quenching. The excimer fluorescence was extremely efficiently quenched by the low CPC concentration in both case. Considering that the quenching requires close contact of fluorophore and the quencher, the extremely efficient quenching implies efficient energies migration to the sites where pyrene groups and CPC quencher are in contact. Hence, this indicates that the preassociated excimer is

located in more hydrophobic microenvironment than monomer probe so that it interacts preferentially with hydrophobic CPC. The effect of CPC on the excimer emission of PNIPAM/NAV/Py-ad is greater than that of PNIPAM/NAV/Py-an, suggesting that the surfactant quencher interacts more strongly with PNIPAM/NAV/Py-ad, which has blocks of hydrophobic pyrene labels, than with PNIPAM/NAV/Py-an. Thus hydrophobic aggregation formed between surfactant CPC and both polymers, even below the critical micelles concentration of CPC. Formation of such aggregate must be the dominant mechanism of fluorescence quenching by CPC.[44, 84]

D. Y. Chu and J. K. Thomas[85] reported that CPC did not show any effect on the opening or closing of polymer chains. This is associated with a binding of this cationic surfactant to both closed and opened polymer chains, a situation where its relative effectiveness in quenching would be similar in both case.

In summary the quenching studies have indicated that hydrophilic cationic quenchers, such as $Fe(aq)^{3+}$ interact much strongly with pyrene labeled distributed homogenously polymer. Hydrophobic quenchers in contrast interact much strongly with blocks of pyrene groups distributed polymer,. Iodide ions is a weak quencher in both case, as a result of electrostatic charge repulsion, especially in basic solutions.

4.0 Conclusion

Pyrene labeled hydrophilic modified PNIPAMs were synthesized by different methods. PNIPAM/NAV/Py-ad prepared by copolymerization with individual monomers possess blockiness of pyrene chromophore, while PNIPAM/NAV/Py-an prepared by post-modification with pyrenyl butylamine has a more random distribution of pyrene chromophore. The LCST of these copolymer are 28.5 and 32.5 °C, respectively, they decrease when pH decrease and can not be observed when pH is higher than 9 (ca.).

Light scattering and fluorescence study indicate that the polymer aqueous solution exist as micelles, the micelle sizes (effective diameter 292 nm for PNIPAM/NAV/Py-ad and 327 nm for PNIPAM/NAV/Py-an, pH=2.50) in acidic condition are much larger than that in basic condition(58 nm for PNIPAM/NAV/Py-ad and 40 nm PNIPAM/NAV/Py-an, pH=9.00). Copolymer chains associated and formed a complex in acidic conditions. This complex formed between carboxylic groups and amide groups either inter- or intrapolymeric chains. They dissociated in basic conditions. The complexation between same type of copolymer was observed in this thesis.

Quenching studies were carried out to investigate the interactions of polymers with cationic, anionic ion, neutral molecule and surfactant. Hydrophilic cationic quenchers, such as $Fe(aq)^{3+}$ interact much more strongly with pyrene labeled distributed homogenously polymer. Hydrophobic quenchers in contrast interact much more strongly with blocks of pyrene groups distributed polymer. Iodide ions is a weak quencher in both cases, as a result of electrostatic charge repulsion, especially in basic solutions. The

interactions with ionic quencher are affected by pH and ionic strength of solution. In both case (cationic and anionic quencher), there exist protected chromophores for PNIPAM/NAV/Py-ad which is inaccessible to these hydrophilic quenchers. Amphiphilic neutral molecules have similar interactions with both copolymers as with PNIPAM. Finaly, a hydrophobic surfactant quencher (CPC) shows much stronger interaction with pyrene excimer than pyrene monomer (10-fold). Quenching studies indicate excimers of pyrene chromophores exist in more hydrophobic microenvironment than that of pyrene monomer.

5. References

1. Hirotsu S.; Irie M. and Dusek K. *Advances in Polymer Science 110* Springer-Verlag Berlin **1993**

2. Casolaro M. *Macromolecules* **1995**, 28, 2351

3. Casolaro M. *Reactive Polymers* **1994**, 23, 71

4. Barbucci R.; Casolaro M.; and Magnani, A.. *Coord. Chem. Rev.* **1992**, 120, 29

5. Chung D. J.; Ito, Y.; ang Imanishi, Y. *J. Controlled Release* **1992**, 18, 45

6. Ishihara K.; Ishimaru N. and Kobayashi M *Polym. J.* **1984**, 16, 625

7. Kost J.; Horbett, T.A.; Ratner B. D. and Singh M.*J. Biomed. Mat. Res.* **1985**, 19, 1117

8. Mika. A. M.; Childs. R. F.; Dickson J. M.; McCarry B. E. and Gaynon D. R. *J. Membrane Sci.* **1995**, 108, 37

9. Plaut H. and Ritter J. J. *J. Am. Chem. Soc.* **1951**, 73, 4076

10. Wooten W. C. Blanton R. B. and Coover H. W. *J. Polym. Sci.* **1957**, 25, 403

11. Tsuchida E. and Abe K. *Advances in Polymer Science 45* Springer-Verlag, Berlin **1982**

12. Bae Y. H.; Okano T. and Kim S. W. *Pharm Res.* **1991**, 8, 531

13. Bae Y. H.; Okano T. and Kim S. W. *J. Polym. Sci. B Polym. Phys.* **1990**, 28, 923

14. Bae Y. H.; Okano T. and Kim S. W. *Makromol Chem. Rapid. Commun.* **1987**, 8, 481

15. Yoshida R.; Sakai K.; Okano T. and Sakurai Y. *Polym. J.* **1991**, 23, 1111

16. Ringsdorf H.; Venzmer J; and Winnik F. M. *Macromolecules* **1991**, 24, 1678

17. Winnik F. M.; *Macromolecules* **1990**, 23, 233

18. Feil H.; Bae Y. B.; Feijen J. and Kim S. W.*Macromolecules* **1993**, 26, 2496

19. Bae Y. H.; Okano T.; and Kim S. W. *Pharm. Res.* **1991**, 8. 531

20. Bae Y. H.; Okano T.; and Kim S. W *J. Polym. Sci. Polym. Phys. Ed.* **1990**, 28, 923

21. Bae Y. H.; Okano T.; and Kim S. W *J. Controlled Release* **1989**, 9, 271

22. Bae Y. H.; Okano T.; and Kim S. W *J. Controlled Release* **1990**, *11, 255*

23. Casolaro M *Polymer*, **1997**, 38, 4215

24. Salamone J. C. *Polymer Materials Encyclopedia* vol. 8, P7979 CRC Press, Boca Raton **1996**

25. Chen G. H. and Hoffman A. S. *Nature* **1995**, 373, 49

26. Dong L. C.; and Hoffman A. S. *J. Controlled. Release.* **1991**, 15, 141

27. Kaneko Y.; SaKai K.; Kikuchi A.; Yoshida R.; Sakurai Y. and Okano T. *Macromolecules* **1995**, 28, 7717

28. Gutowska A.; Bae Y. H.; Feijen J.; Kim S. W. *Macromolecules* **1994**, 27, 4167

29. Gutowska A.; Bae Y. H.; Feijen J.; Kim S. W. *J. Controlled. Release.* **1992**, 22, 95

30. Gutowska A.; Bae Y. H.; Jacobs H.; Mohammad F.; Mix D.; Feijen J. and Kim S. W. *J. Biomed. Mat. Res.* **1995**, 29, 811

31. Eisele U. *Introduction to Polymer Physics* Springer-Verlag **1990**

32. Osada Y.; Sato. M. *Polymers* **1980**, 21, 1057

33. Frank A.; *Makromol. Chem.* **1966**, 96, 258

34. Abe K.; Ohno H.; Nii A. and Tsuchida E. *Makromol. Chem.* **1978**, 179, 2043.

35. Bosscher F.; Keeksta G.; Challa G. *Polymer* **1981**, 22, 124

36. Sivadasan K. Somasundaran P. *J. Polym. Sci. A Polym. Chem.* **1991**, 29, 911. b) Maltesh C.; Somasundaran P.; Pradip; Kulkarni R. A.; and Gundiah S. *Macromolecules* **1991**, 24, 5775.

37. Pradip; Maltesh C.; Somasundaran P.; Kulkarni R. A. and Gundiah S. *Langmuir* **1991**, 7, 2108

38. Tjipangandjara K. F. and Somasundaran P. *Colloids and Surfaces* **1991**, 55, 245

39. Kiefer. J. J.; Somasundaran P.; and Ananthapadmanabhan K. P. *Langmuir* **1993**, 9, 1187

40. a)Oyama H. T.; Tang W. T. and Frank C. W. *Macromolecules* **1987**, 20, 1839.b) Oyama H. T.; Tang W. T. and Frank C. W. *Macromolecules*, **1987**, 20, 474

41. Wang Q.; He L. Y. *Polymer* **1997**, 38, 3931

42. Itagaki H.; Horie K.; and Mita I. *Prog. Polym. Sci.* **1990**, 15, 361.b) Horie K.; Hirao A.; Kawabata J.; Mita I.; Nakahama S. and Yamazaki N. *Polym. J.* **1980**, 12, 319

43. Kosower E. M.; Dodiuk H.; Tanizawa K.; Ottolenghi M. and Orbach N. *J. Am. Chem. Soc.* **1975**, 97, 2167

44. Wang Y.; and Morawetz H. *Macromolecules* **1989**, 22, 167

45. Winnik F. M. *Chem Rev.* **1993**, 93, 587

46. a)Schild H. G. and Tirrell D. A. *Langmuir* **1991**, 7, 1319. b) Schild H. G. and Tirrell D. A *Macromolecules* **1992**, 25, 4553

47. Ezzell S. A. and McCormick C. L. *Macromolecules*, **1992**, 25, 1881

48. Ezzell S. A. Hoyle C. E.; Creed D.; and McCormick C. L. *Macromolecules*, **1992**, 25, 1887

49. a)Barbucci R.; Carolaro M.; Magnani A. and Ronrolini C. *Macromolecules* **1991**, 24, 1249. b) Barbucci R.; Carolaro M.; Ferruti P. and Magnani A. *Polymer* **1989**, 30, 1751. c) Casolaro. M and Barbucci. R. *Collo. and Surfan. A Physicochem. and Eng.* **1993**, 77, 81

65. Chen T. S. and Thomas J. K *J. Polym. Sci. Polym, Chem. Edit.* **1979**, 17, 1103

66. Turro N. J. and Arora K. S. *Polymer* **1986**, 27, 783

67. Kramer M. C.; Welch C. G.; Steger J. R. and McCormick C. L. *Macromolecules* **1995**, 28, 52248

68. Wang Q.; He L. Y. *J. Functional Polym.* **1996, *9, 78***

69. Oyama H. T.; Hemker D. J. and Frank C. W. *Macromolecules* **1989**, 22, 1255

70. Lakowicz J. R. *Principles of Fluorescence Spectroscopy* Plenum Press, New York **1983**

71. Manning G. S. *J. Chem. Phys.* **1965**, 43, 4250

72. Manning G. S. *J. Chem. Phys.* **1965**, 43, 4260

73. Morishima Y.; Ohgi H. and Kamachi M. *Macromolcules* **1993**, 26, 4293

74. Morishima Y; Sato T and Kamachi M *Macromolecules* **1996**, 29, 1633

75. Morishima Y.; Kobayashi T. and Nozakura S. I. *Macromolecules* **1988**, 21, 101

76. Morrison M. E.; Dorfman R. C.; Clendening W. D.; Kiserow D. J.; Rossky P. J. and Webber S. E. *J. Phys. Chem.* **1994**, 98, 5534.

77. Johanson, L.; Elvingson C. and Löfroth J. *Macromolecules,* **1991**, 24, 6024

78. Turro, N. J.; Barton J. K. and Tomalia D. A. *Acc. Chem. Res.* **1991**, 21, 332

79. Yekta A.; Duhamel J. Winnik M. A. *J. Chem. Phys.* **1990**, 97, 1554

80. Taha I. S. and Morawetz H. *J. Am. Chem. Soc.* **1971**, 829

81. Winnik F. M. *Macromolecules* **1990**, 23, 1647

82. Deumie M.; Baraka M. E.; and Quinones E. *J. photochem. Photobio. A: Chem.* **1995**, 87, 105

83. Faes H.; Schryver F. C. Sein A.; Bijma K.; Kevelam J.; and Engberts J. B. F. N. *Macromolecules* **1996**, 29, 3875

50. Kubota K.; Fujishige S.; and Ando I. *Polym. J.* **1990**, 22, 15. b) Demas J. N. and Crosby G. A. *J. Phys, Chem.* **1971**, 75, 991. c)Stuart B. and Ando D. J. *Modern Infrared Spectroscopy* New York, Wiley **1996**

51. a) Mika A. M.; Childs F. R.; et al. to be published b) Barbucci, R.; Casolaro M.; Danzo N.; Barone V. Ferruti P. and Angelon A *Macromolecules* **1983**, 16, 456 c) Gregor H. P. and Frederick M. *J.Polym. Sci.* **1957**, 23, 451. d) Serjeant E. P. *Potentiometry and Potentiometric Titration* New York, Wiley **1984**

52. Lewis O. G. *Physical Constants of Linear Homopolymers* Springer-Verlag **1968**

53. Smidsrod O. *Macromolecules* **1969**, 2, 272

54. Schild H. G *Prog. Polym. Sci.* **1992**, 17, 163

55. Winnik F. M.; Adronov A. and Kitano H. *Can. J. Chem.* **1995**, 73, 030

56. Fujishige S.; Kubata K. and Ando I. *J. Phys. Chem.* **1989**, 93, 3311

57. Molyneux P. *Water-soluble Synthetic Polymers: Properties and Behavior vol. 2* CRC Press , Boca Raton **1983**

58. Kiler J.; Scraton A. B.and Peppas N. A.; *Macromolecules* **1990**, 23, 4944

59. Katono H.; Ogata N.; Okano T. and sakurai Y. *Polym. J.* **1991**, 23, 1179

60. Schild H. G. and Tirrell A. *J. Phys. Chem.* **1990**, 94, 4352?

61. Degiorgio V. and Corti M. *Physics of Amphiphiles: Micelles, Vesicles and Microemulsion* North Holland **1985**

62. Huglin M. B. *Light Scattering from Polymer Solution* Academic Press, London **1972**

63. Turro, N. J. *Modern Molecular Photochemistry* The Benjamin/Cummings Publishing Co., Inc. **1978**

64. Tanford C. *The Hyfrophobic effect: Formation of micelles and Biological membranes* John Wiley & Sons, New York **1973**

84. Chen T. S. and Thomas J. K *Macromolecules* **1984**, 17, 2142

Scheme 3a Preparation of *N*-acryloyl-*L*-valine

$$L\text{-Valine} \quad \xrightarrow[\text{NaOH}]{\text{CH}_2\text{CHCOCl}} \quad \xrightarrow{\text{HCl}} \quad$$

$$\begin{array}{c} \overset{f}{H} \\ \overset{f}{H} \end{array} \!\! C = CH^e$$

$$| \\ C = O \\ | \\ NH^d \\ | \\ \overset{c}{C}HCOOH \\ | \\ \overset{b}{C}H(\overset{a}{C}H_3)_2$$

NAV

Oxalyl Chloride

1

2

NH₃. H₂O

$CH_2CH_2CH_2CH_2NH_2 \cdot HCl$

1) LiAlH₄/THF

2) HCl

$CH_2(CH_2)_2 CONH_2$

4

3

Acryloyl Chloride

Et₃N/CH₂Cl₂

$CH_2CH_2CH_2CH_2NHCOCH= CH_2$

Compound 5
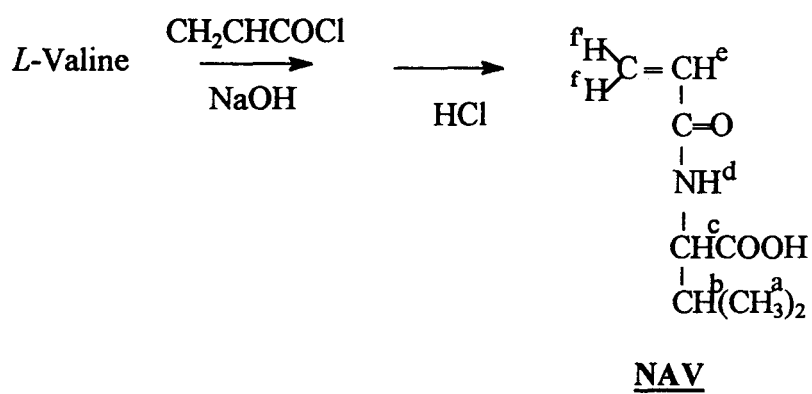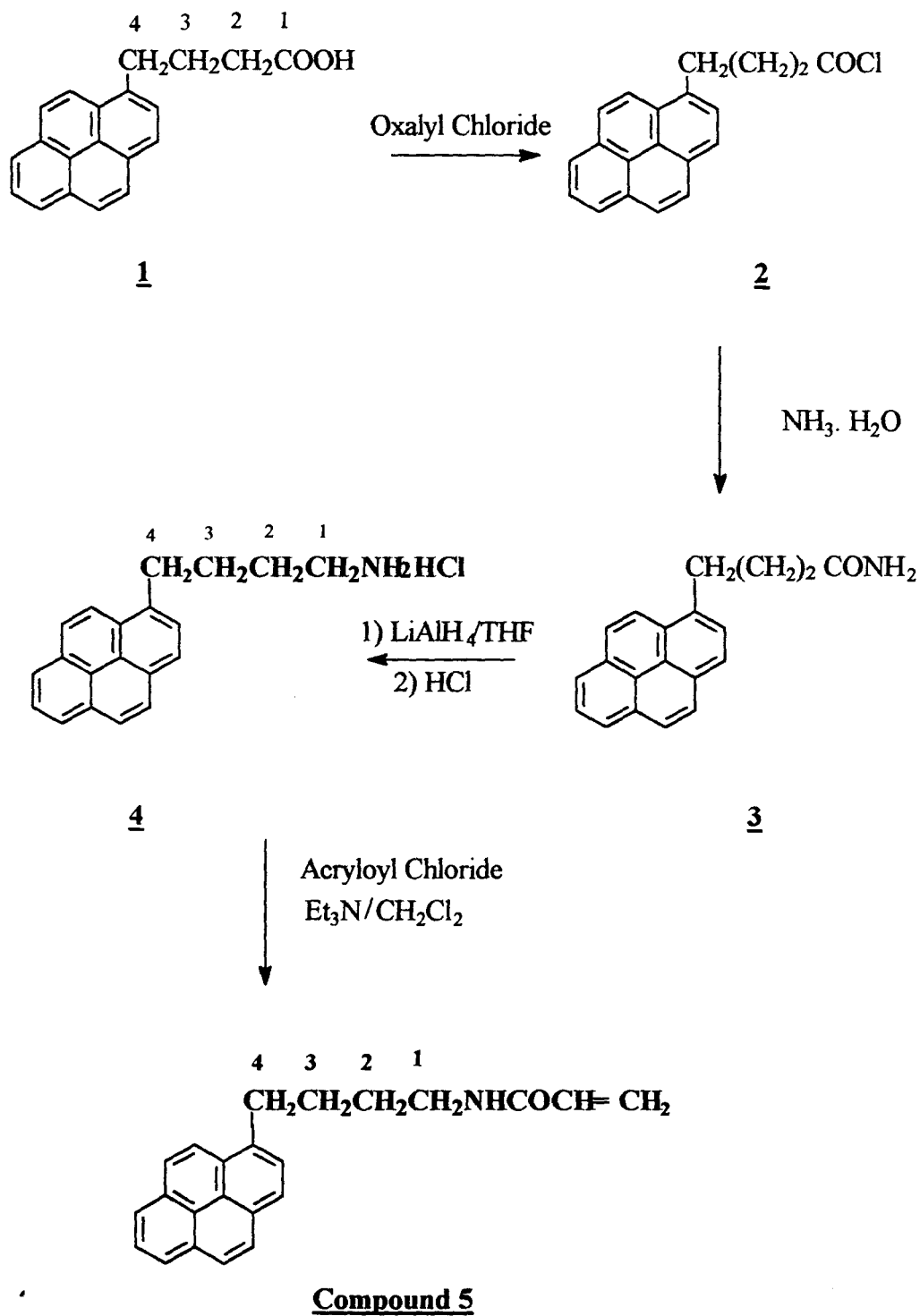
Scheme 4: Preparation of Copolymers

Copolymer
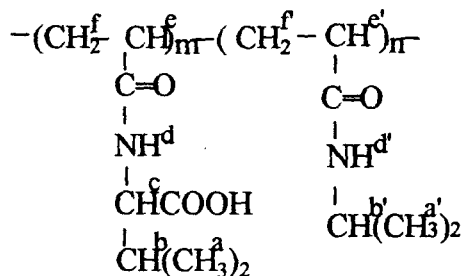
$-(CH_2^f-CH^e)_m-(CH_2^{f'}-CH^{e'})_n-$
|$\quad\quad\quad$|
C=O$\quad\quad\quad$C=O
|$\quad\quad\quad\quad$|
NH$^d\quad\quad\quad\quad$NH$^{d'}$
|$\quad\quad\quad\quad\quad$|
CHCOOH$\quad\quad$CH(CH_3)_2^{b'a'}
|^c
CH(CH_3)_2^{b\;a}

Reactive Copolymer

↑ AIBN/Dioxane
$\quad$ Polymerization

NAV + NIPAM $\quad$ *N*-acryloxy-succinimide
$\longrightarrow$
$\quad\quad\quad\quad\quad\quad$ AIBN/Dioaxane

$\quad\quad\quad$ Compound 5
↓
$\quad\quad\quad$ AIBN/Dioxane

$-(CH_2-CH)_m-(CH_2-CH)_n-(CH_2-CH)_x-$
|$\quad\quad\quad\quad$|$\quad\quad\quad\quad$|
C=O$\quad\quad\quad\quad$C=O$\quad\quad\quad\quad$C=O
|$\quad\quad\quad\quad\quad$|$\quad\quad\quad\quad\quad$O
NH$\quad\quad\quad\quad\quad$NH$\quad\quad\quad\quad$|
|$\quad\quad\quad\quad\quad\quad$|$\quad\quad\quad$O=N=O (succinimide)
CHCOOH$\quad\quad\quad$CH(CH_3)_2
|
CH(CH_3)_2

$\quad\quad\quad\quad\quad\quad\quad\quad$ 1)Pyrenyl butylamine hydrochlorid
$\quad\quad\quad\quad\quad\quad\quad\quad$ 2)*N*-iso-propylamine

$-(CH_2-CH)_m-(CH_2-CH)_n-(CH_2-CH)_x-$
|$\quad\quad\quad\quad$|$\quad\quad\quad\quad$|
CO$\quad\quad\quad\quad$CO$\quad\quad\quad\quad$CO
|$\quad\quad\quad\quad$|$\quad\quad\quad\quad$|
NH$\quad\quad\quad\quad$NH$\quad\quad\quad\quad$NH
|$\quad\quad\quad\quad\quad$|$\quad\quad\quad\quad$|
CHCOOH$\quad\quad$CH(CH_3)_2$\quad$(CH_2)_4
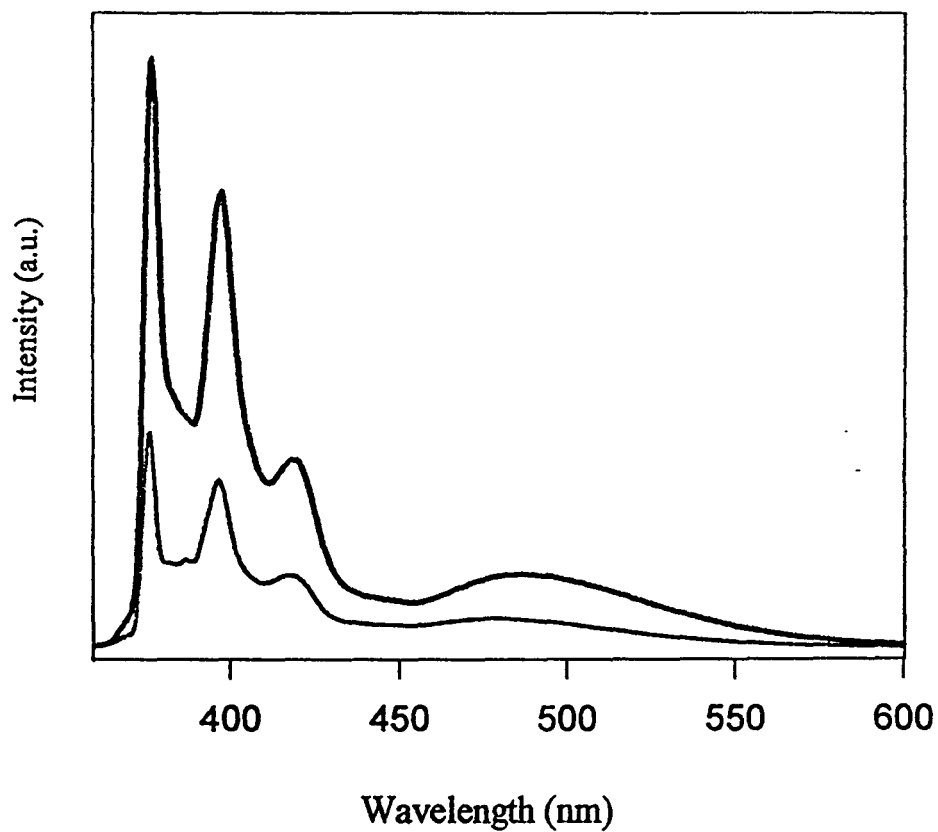|
CH(CH_3)_2
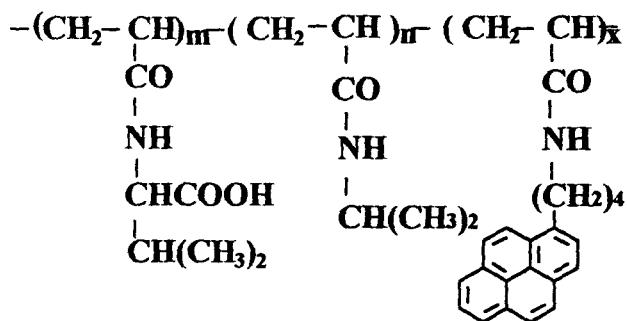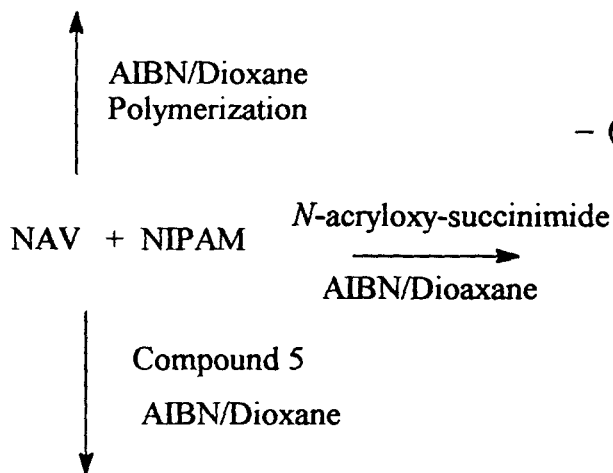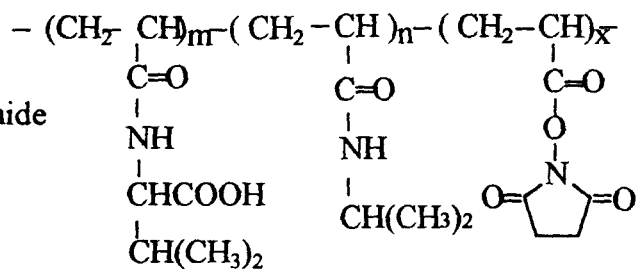
Labeled Copolymer
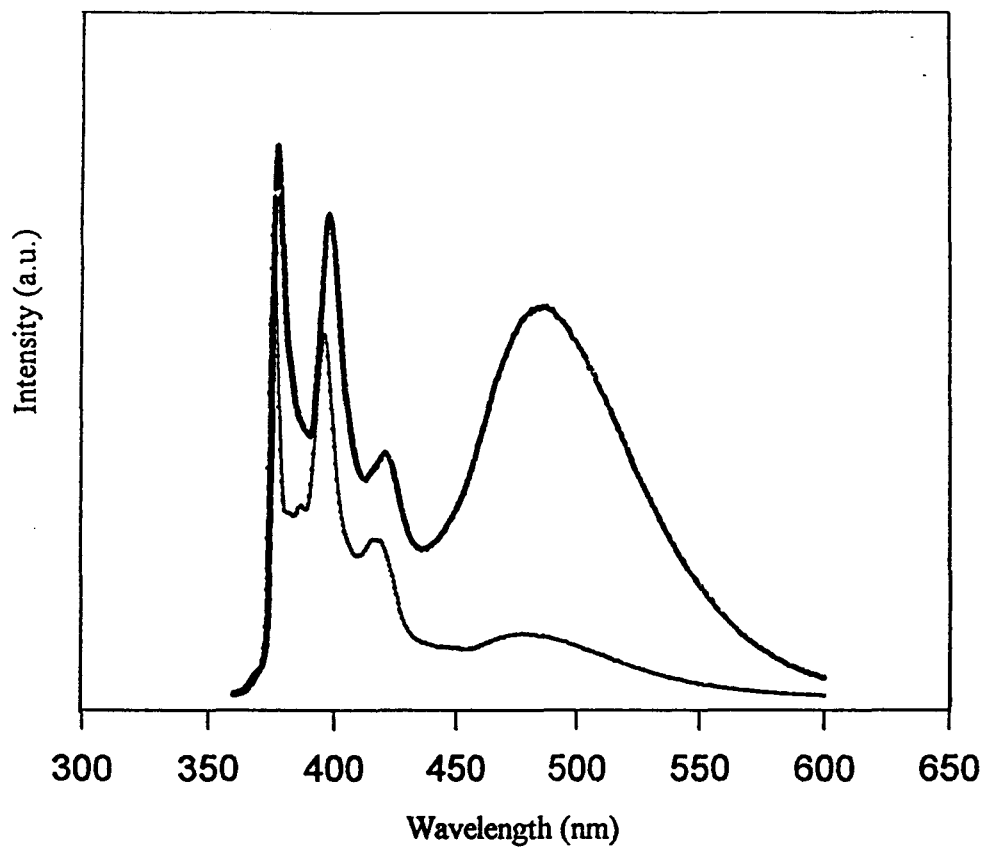
Figure 1: Fluorescence emission spectra of PNIPAM/NAV/Py-ad in water and methanol, excitation wavelength 346 in water (thick line), 342 nm in methanol (thin line), 25 °C.
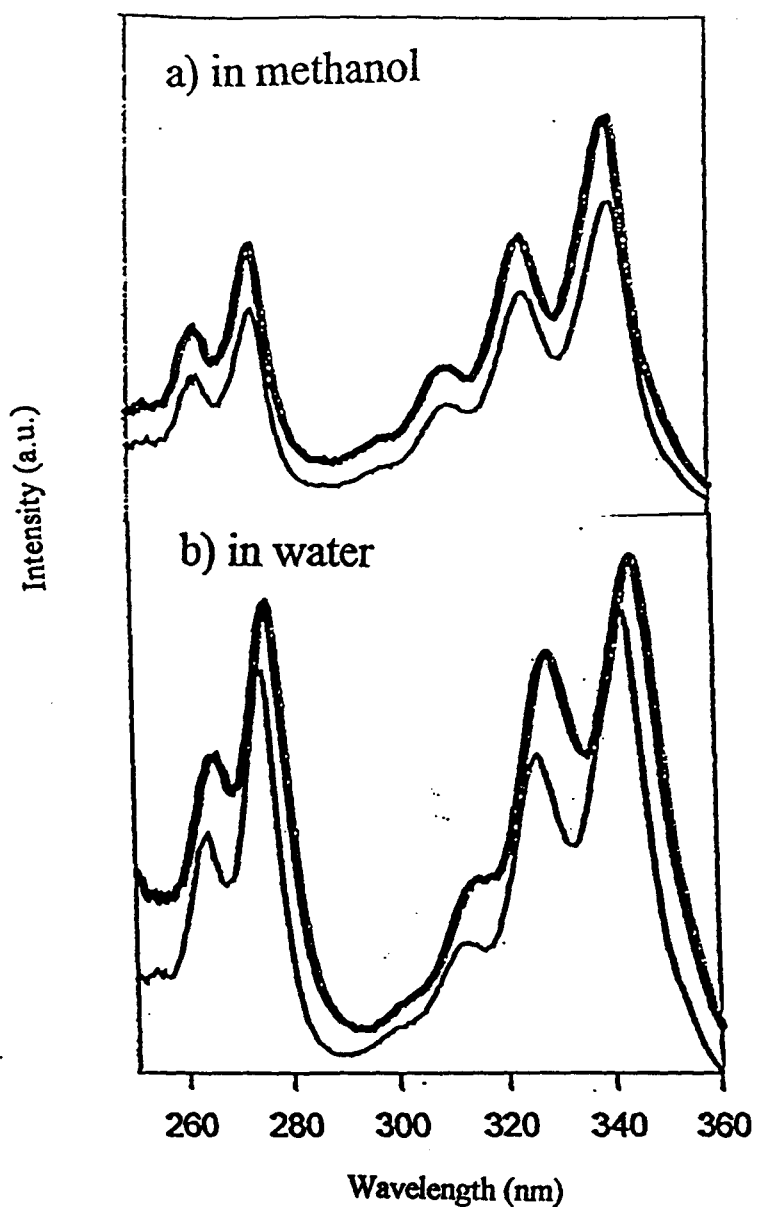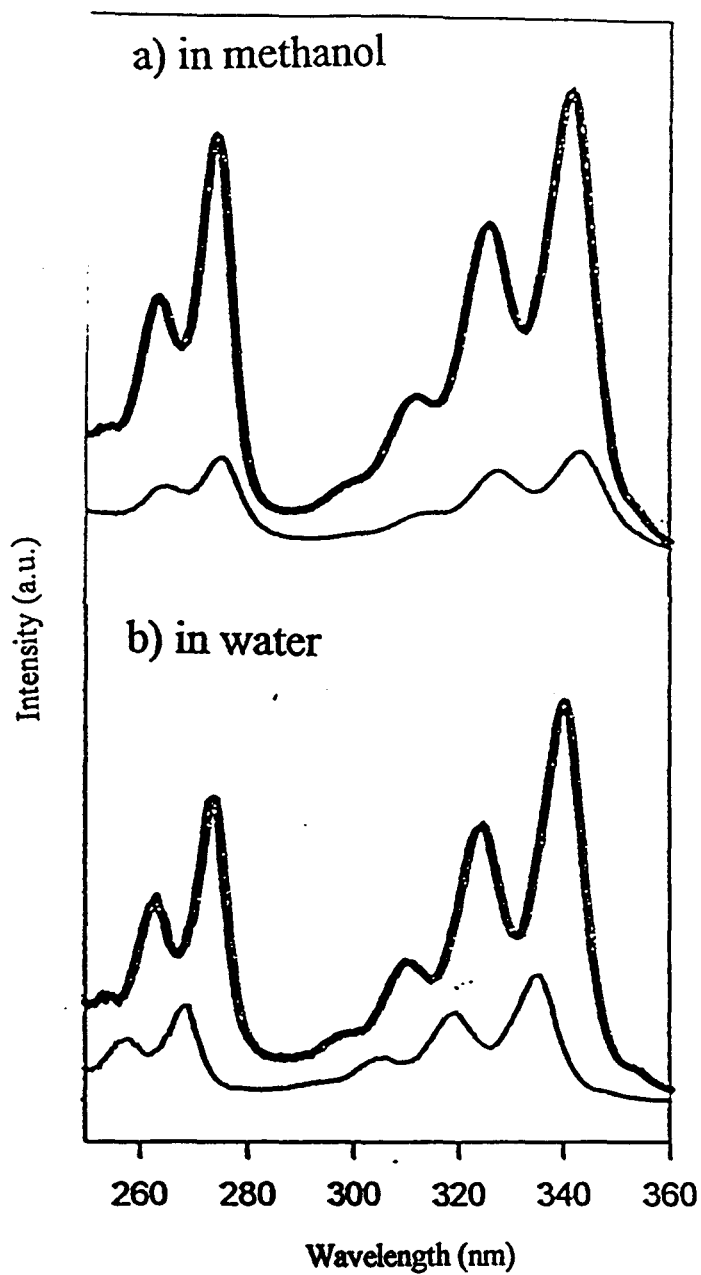
Figure 2: a) Excitation spectra of PNIPAM/NAV/Py-ad in methanol, monomer emission wavelength 391 (thick line), excimer emission wavelength 481nm (thin line); b) Excitation spectra of PNIPAM/NAV/Py-ad in water, excimer emission wavelength 486 (thick line), monomer emission wavelength 391 nm (thin line), 25 °C
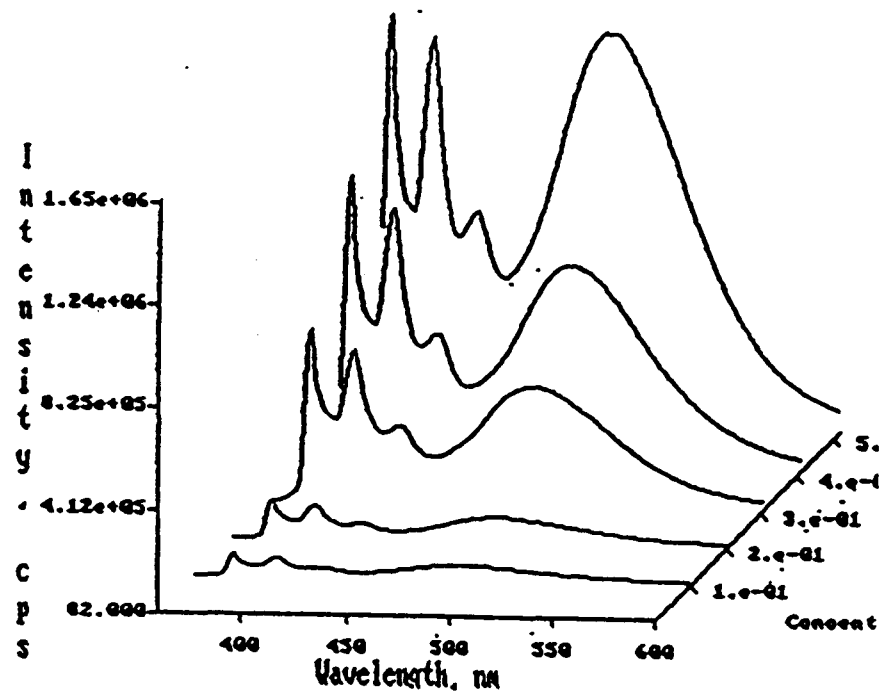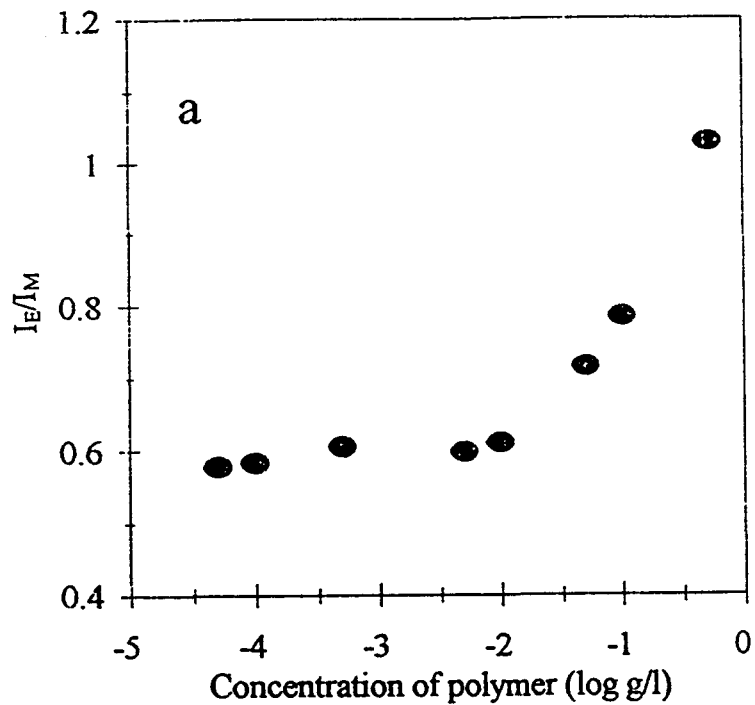
Figure 3: a) Plot of the excimer to monomer emission intensities ratio (I_E/I_M) as a function of polymer concentration for aqueous solution of PNIPAM/NAV/Py-ad; b) Fluorescence spectra   of PNIPAM/NAV/Py-ad   measured at several polymer concentration between 5×10^{-5} and 0.51 g/l, 25°C, $\lambda_{exc} = 346$nm.
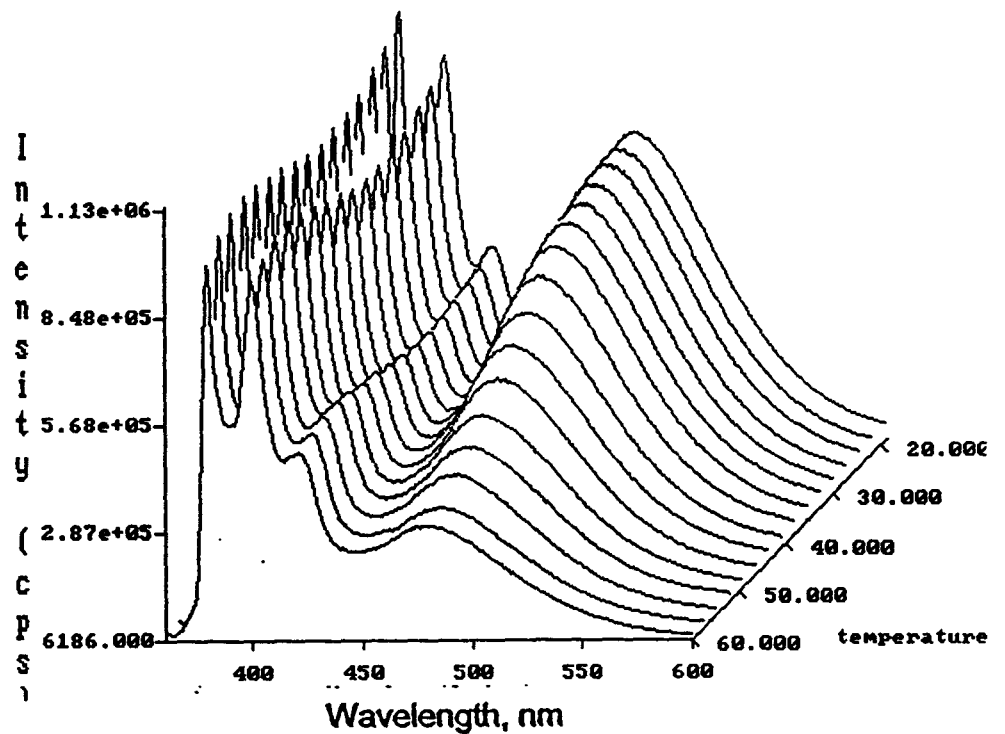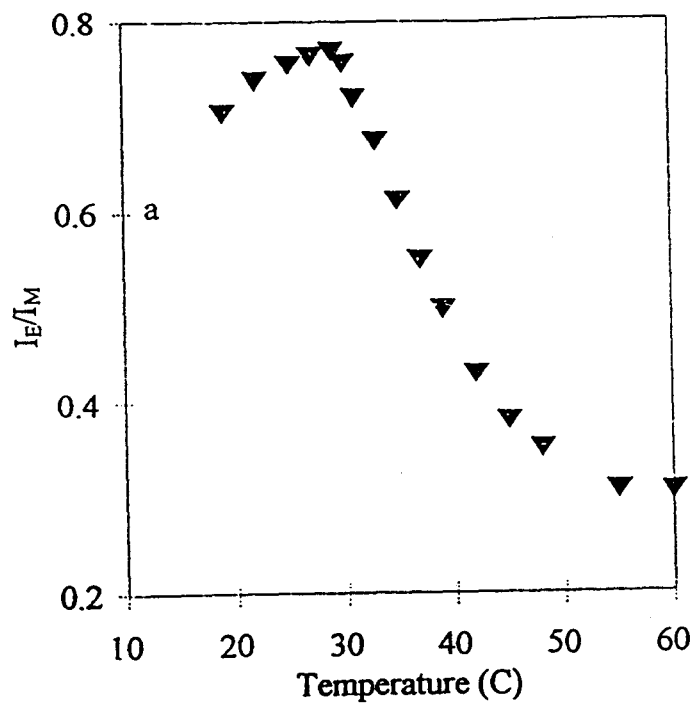
Figure 4: a) Plot of the excimer to monomer emission intensities ratio (I_E/I_M) as a function of temperature for aqueous solution of PNIPAM/NAV/Py-ad; b) Fluorescence spectra of PNIPAM/NAV/Py-ad measured at several temperature between 15 and 60°C, polymer concentration 0.1g/l, λ_{exc} = 346nm.
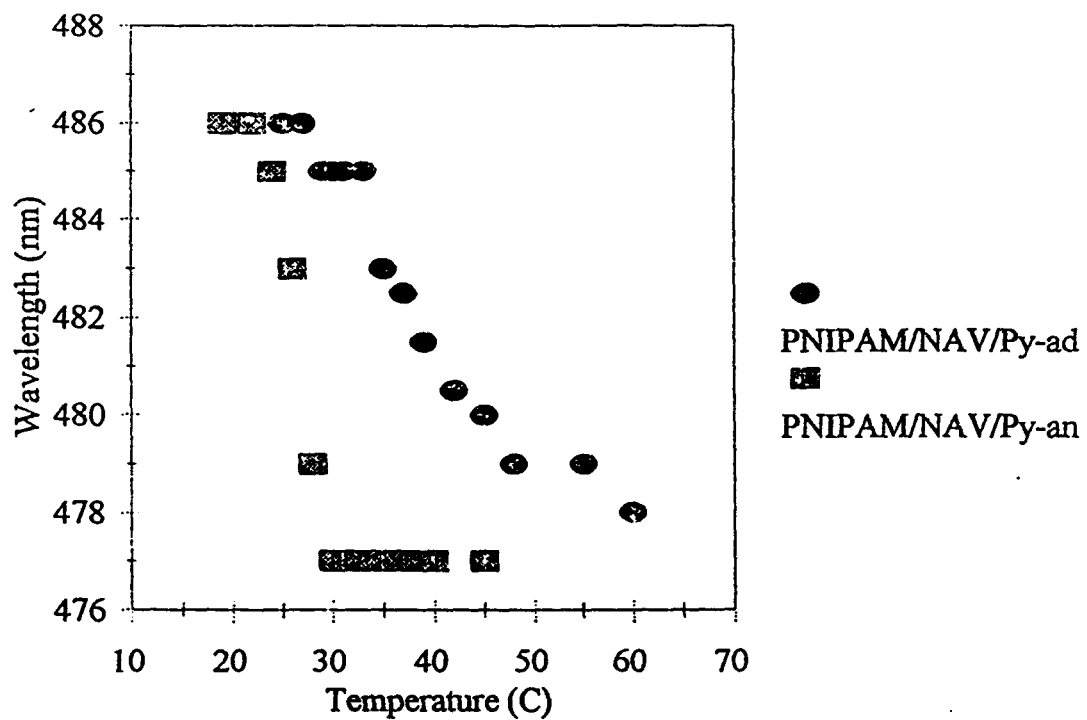
Figure 5: Plot of maximum of excimer wavelength as a function of temperature, polymer concentration for PNIPAM/NAV/Py-ad: 0.1g/l, and PNIPAM/NAV/Py-an: 0.43g/l, excitation wavelength 346 nm.
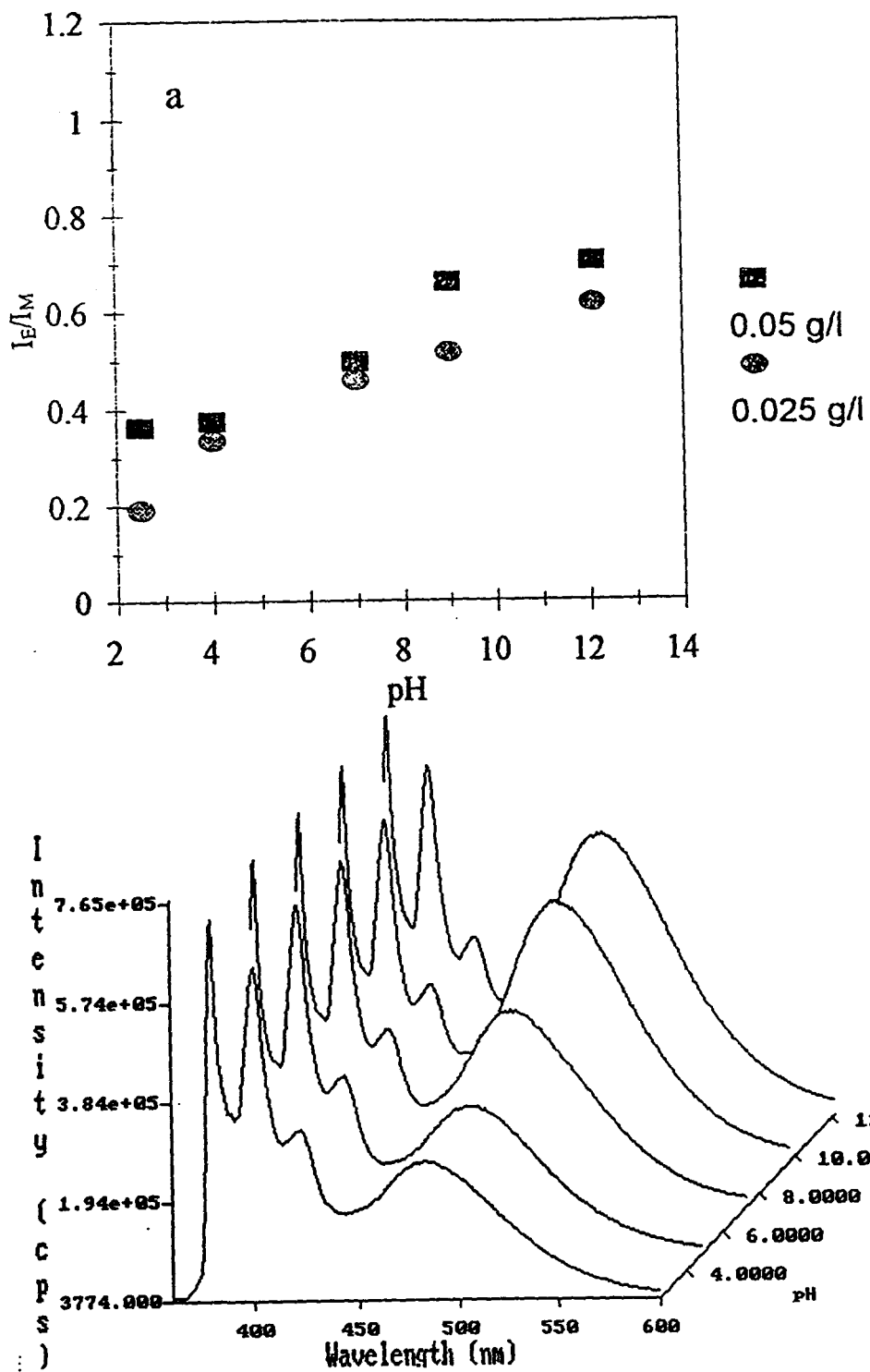
Figure 6: a) Plot of the excimer to monomer emission intensities ratio (I_E/I_M) as a function of pH for buffer solution of PNIPAM/NAV/Py-ad; b) Fluorescence spectra of PNIPAM/NAV/Py-ad measured at several pH between 2.5 and 12.1, polymer concentration 0.025 and 0.05g/l, 25°C, $\lambda_{exc} = 346$nm.
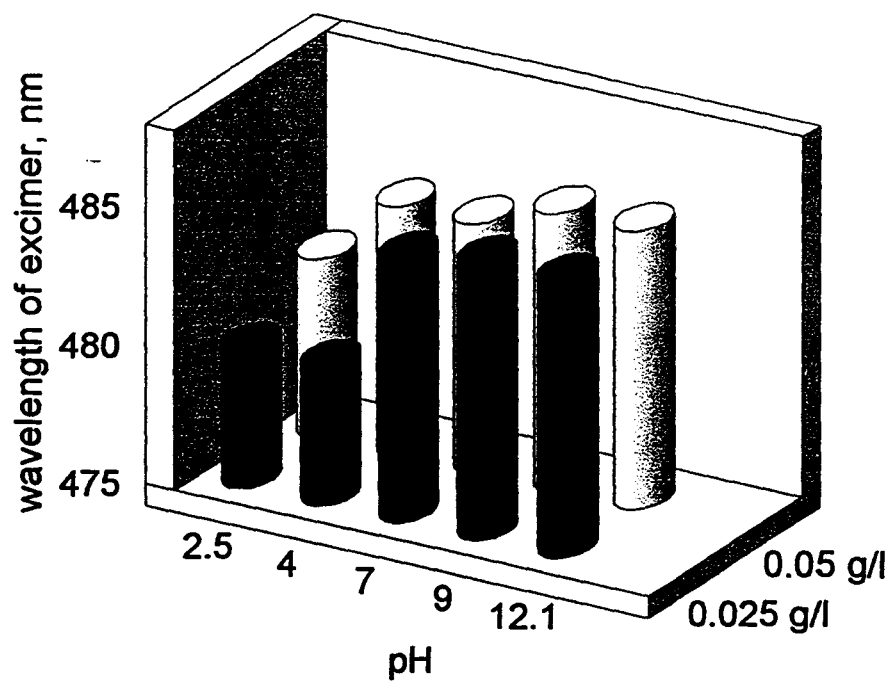
Figure 7: Plot of maximum of excimer wavelength of PNIPAM/NAV/Py-ad as a function of pH, polymer concentration 0.025 and 0.05g/l, 25°C, λ_{exc} = 346nm.

P17   in water and methanol

Figure 8: Fluorescence emission spectra of PNIPAM/NAV/Py-an in water and methanol, excitation wavelength 344 in water (thick line), 342 nm in methanol (thin line), 25 °C.

a) in methanol

b) in water

Intensity (a.u.)

Wavelength (nm)

260   280   300   320   340   360

Figure 9: Excitation spectra of PNIPAM/NAV/Py-an. a) in methanol, monomer emission wavelength 391 (thick line), excimer emission wavelength 481nm (thin line); b) in water, monomer emission wavelength 391 (thick line), excimer emission wavelength 486nm (thin line); 25 °C.
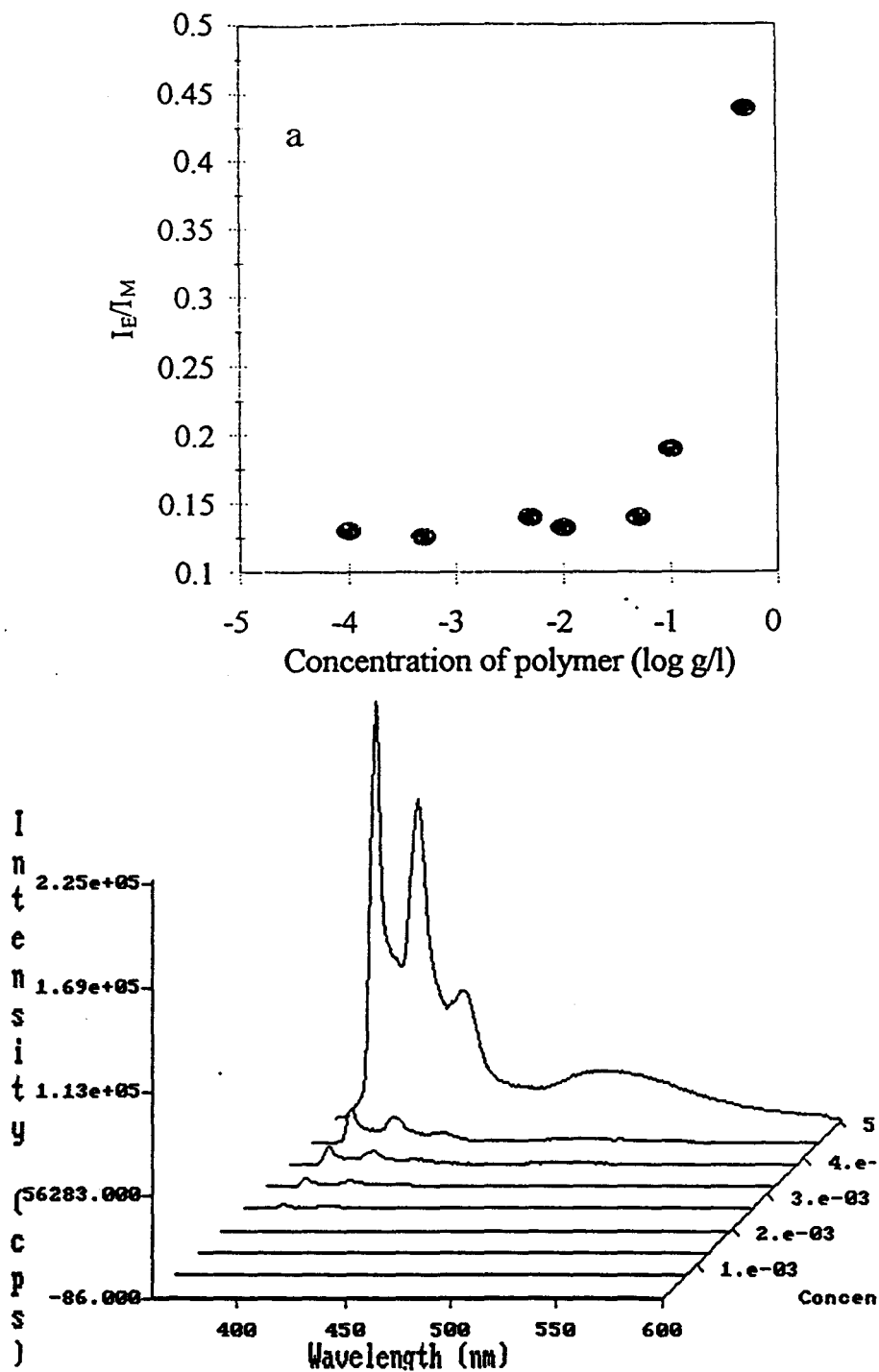
Figure 10: a) Plot of the excimer to monomer emission intensities ratio (I_E/I_M) as a function of polymer concentration for aqueous solution of PNIPAM/NAV/Py-an; b) Fluorescence spectra of PNIPAM/NAV/Py-an measured at several polymer concentrations between 10^{-4} and 0.44 g/l, 25°C, λ_{exc} = 344nm.
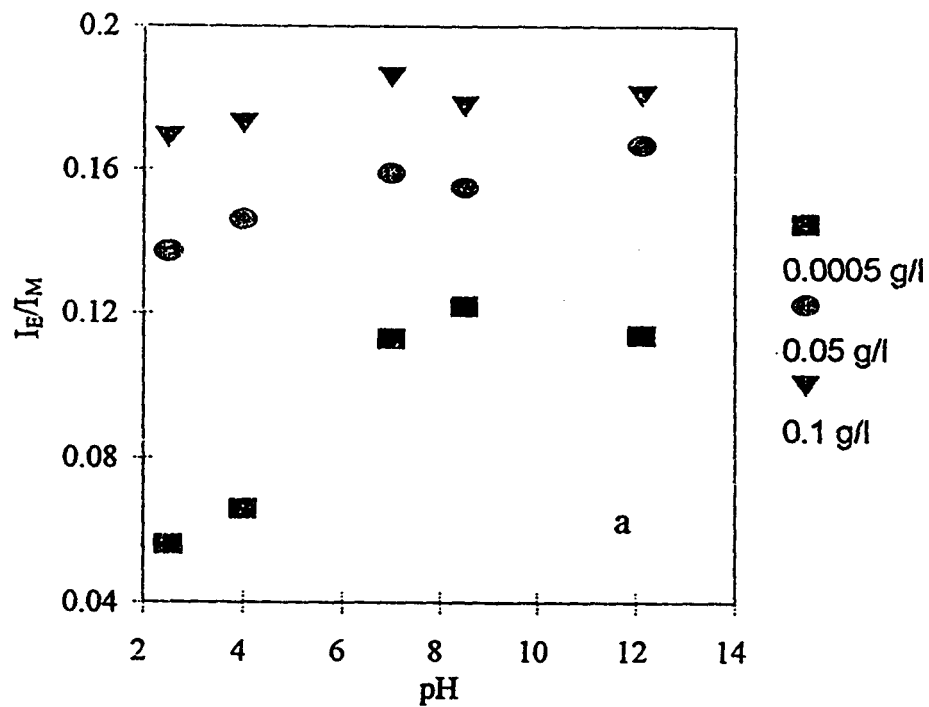
Figure 11: a) Plot of the excimer to monomer emission intensities ratio (I_E/I_M) as a function of pH for buffer solution of PNIPAM/NAV/Py-an; b) Fluorescence spectra of PNIPAM/NAV/Py-an measured at several pH between 2.5 and 12.1, 25°C, λ_{exc} = 344nm.
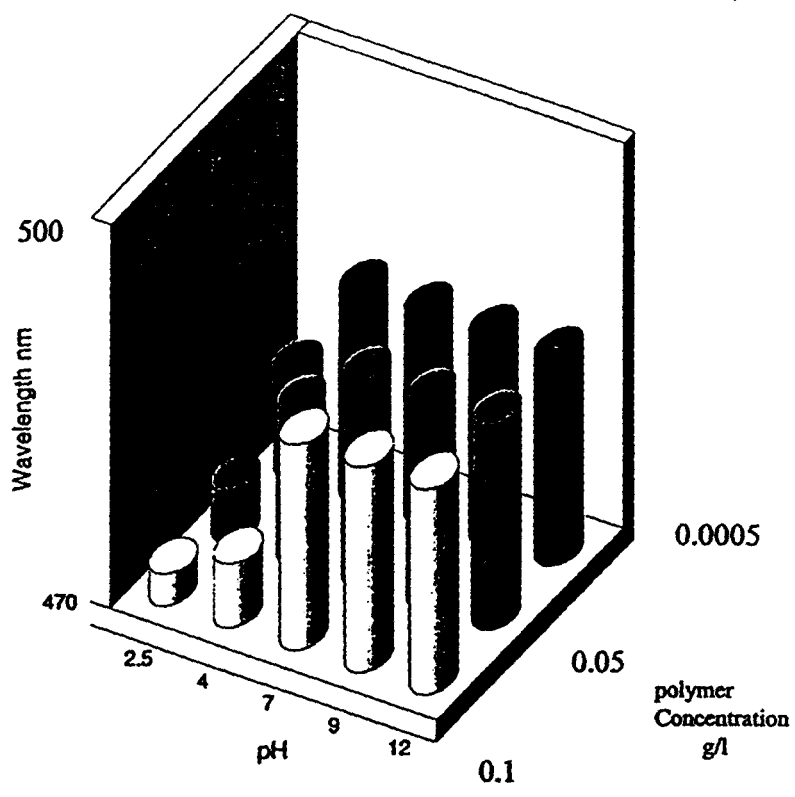
Figure 12: Plot of maximum of excimer wavelength of PNIPAM/NAV/Py-an as a function of pH, 25°C, $\lambda_{exc} = 344$nm.
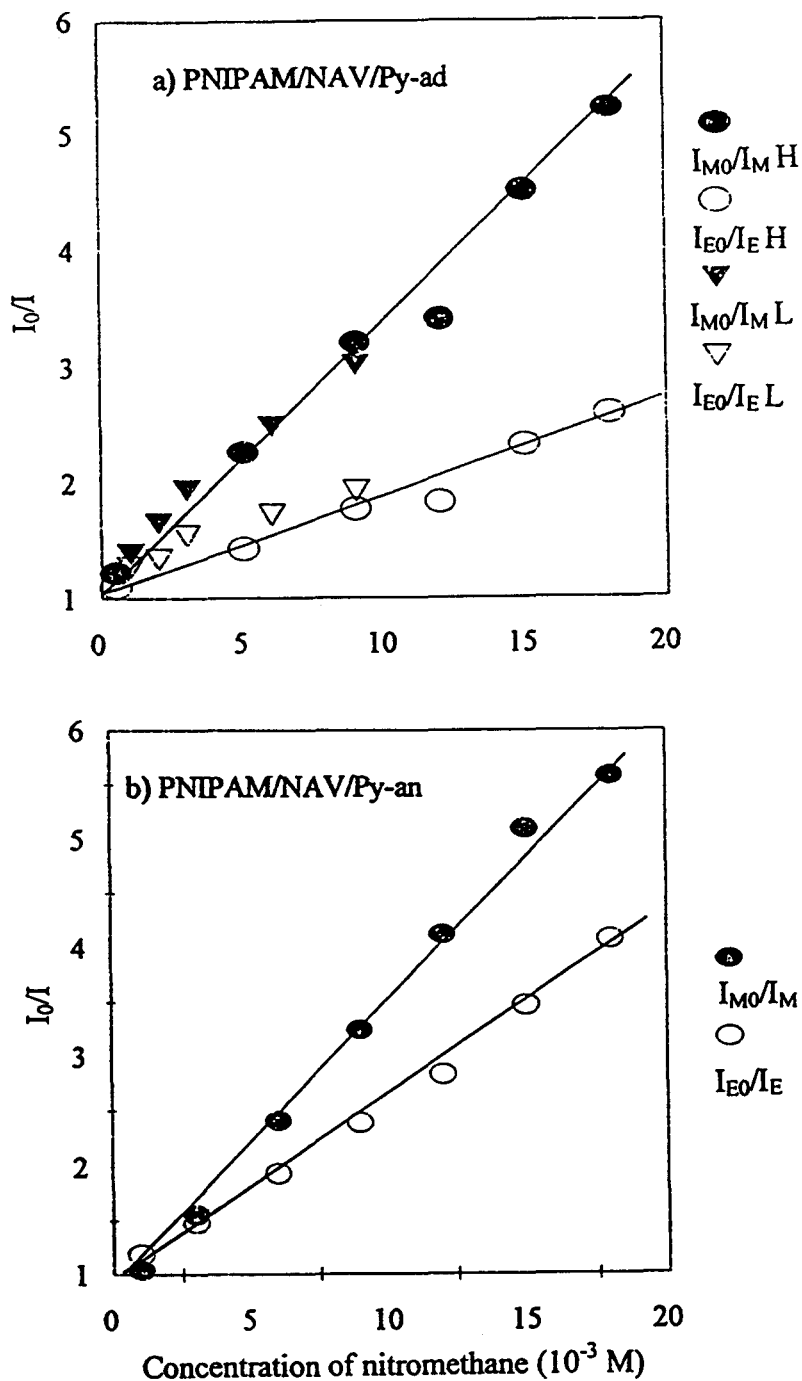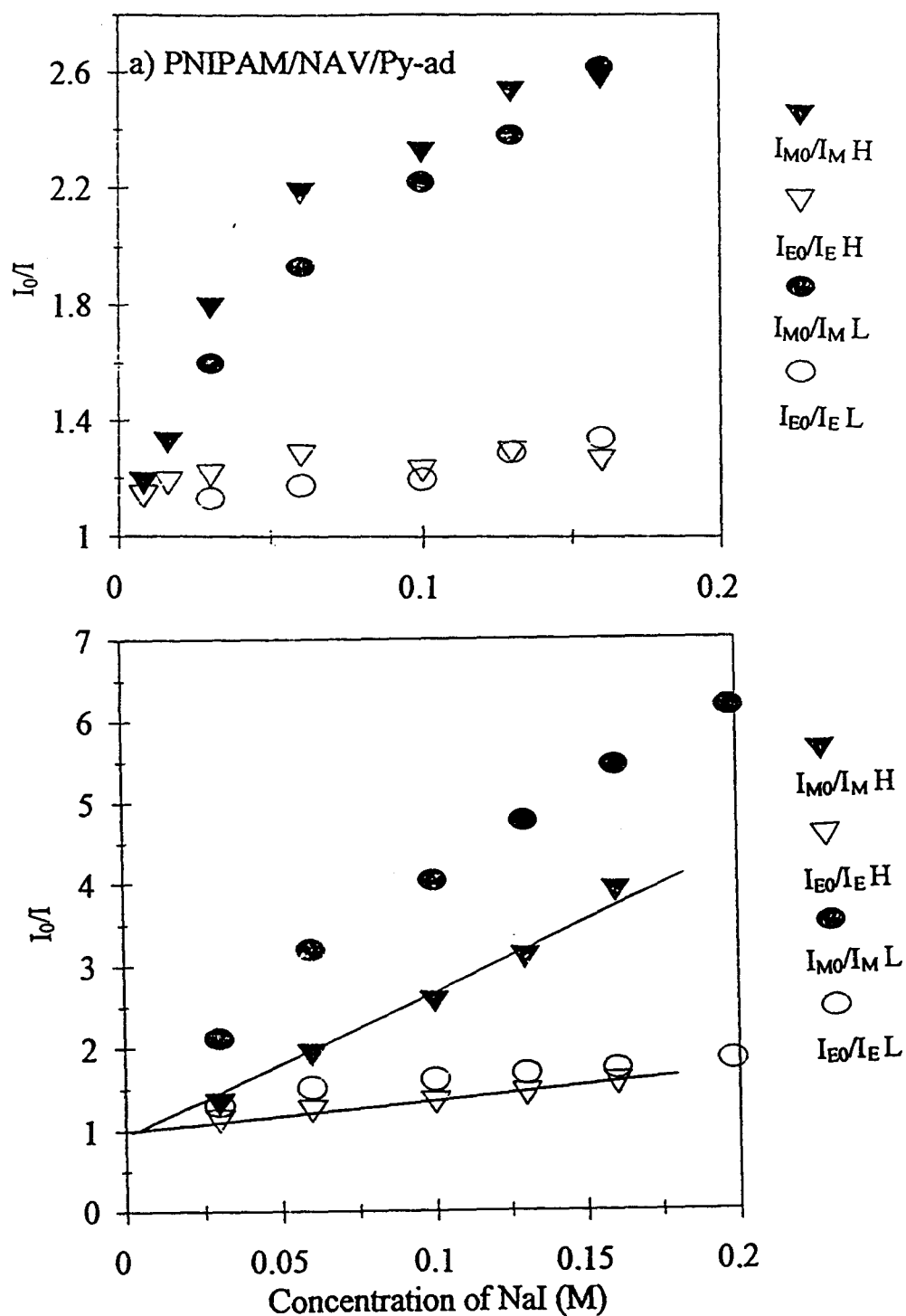
Figure 13: Ratio of I_0/I pyrene monomer emission intensities (solid circle) and excimer emission intensities (circle) in the absence and in the presence of nitromethane in copolymer aqueous solutions as a function of nitromethane concentrations, polymer concentration 0.05g/l, 25°C. a) PNIPAM/NAV/Py-ad, λ_{exc} = 346nm; b) PNIPAM/NAV/Py-an, λ_{exc} = 344nm.
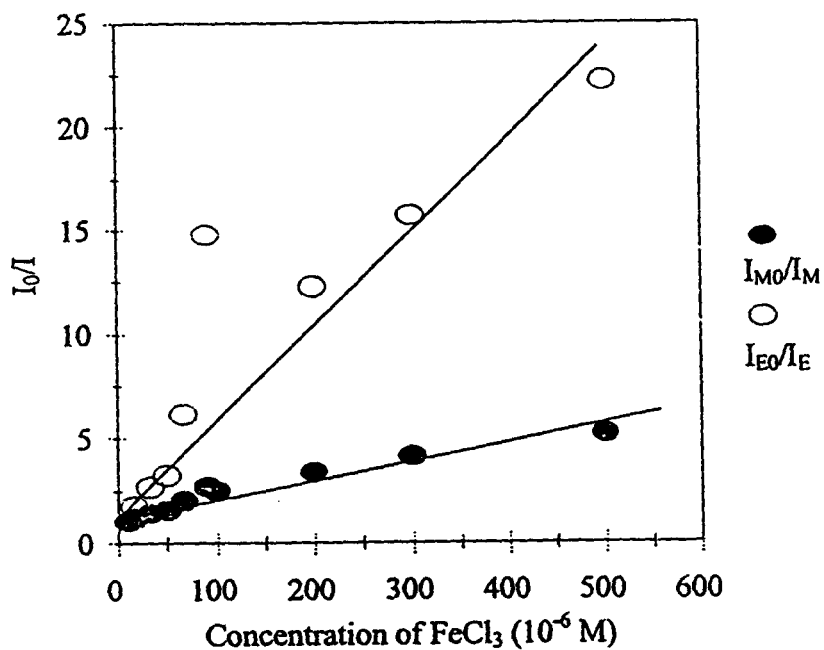
Figure 14: Ratio of I_0/I pyrene monomer emission intensities (solid circle) and excimer emission intensities (circle) in the absence and in the presence of FeCl$_3$ in PNIPAM/NAV/Py-an aqueous solutions as a function of FeCl$_3$ concentrations, polymer concentration 0.05g/l, 25°C, λ_{exc} = 344nm.
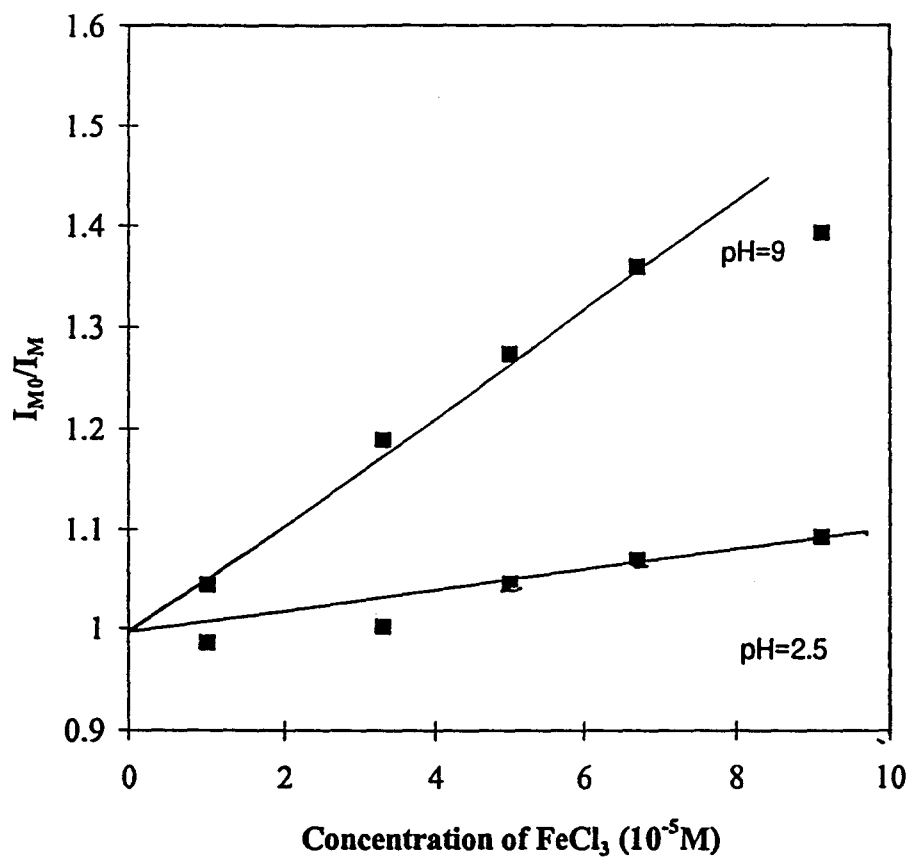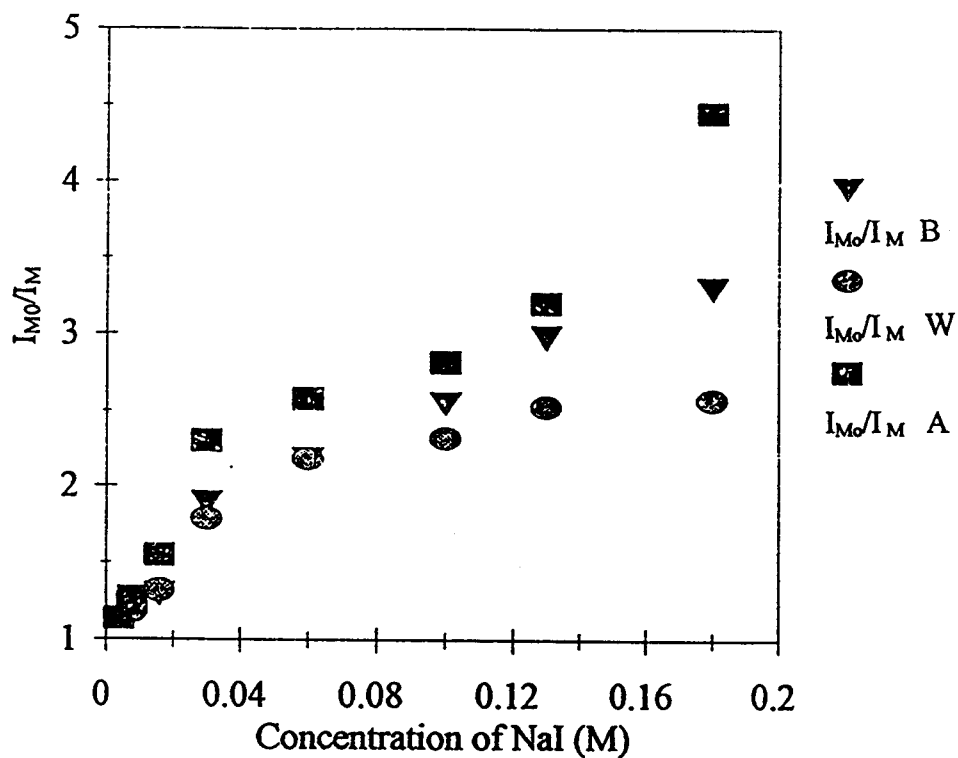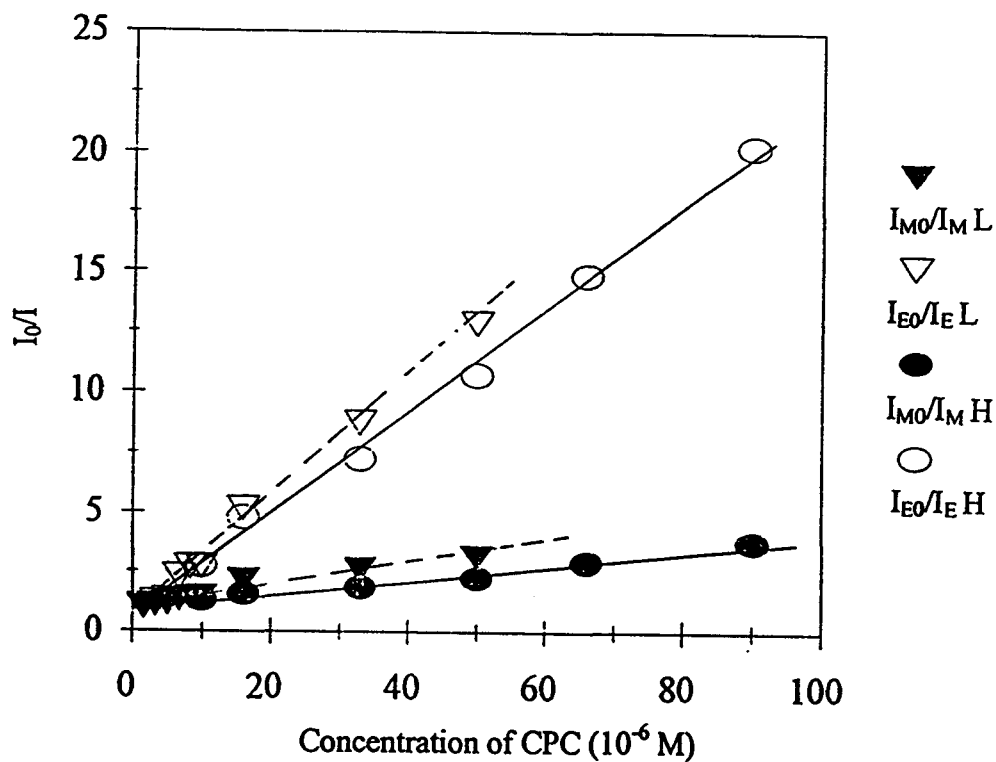
Figure 15: Ratio of I_0/I pyrene monomer emission intensities in the absence and in the presence of $FeCl_3$ in PNIPAM/NAV/Py-an buffer solutions as a function of $FeCl_3$ concentrations, polymer concentration 0.05g/l, 25°C, $\lambda_{exc} = 346nm$.
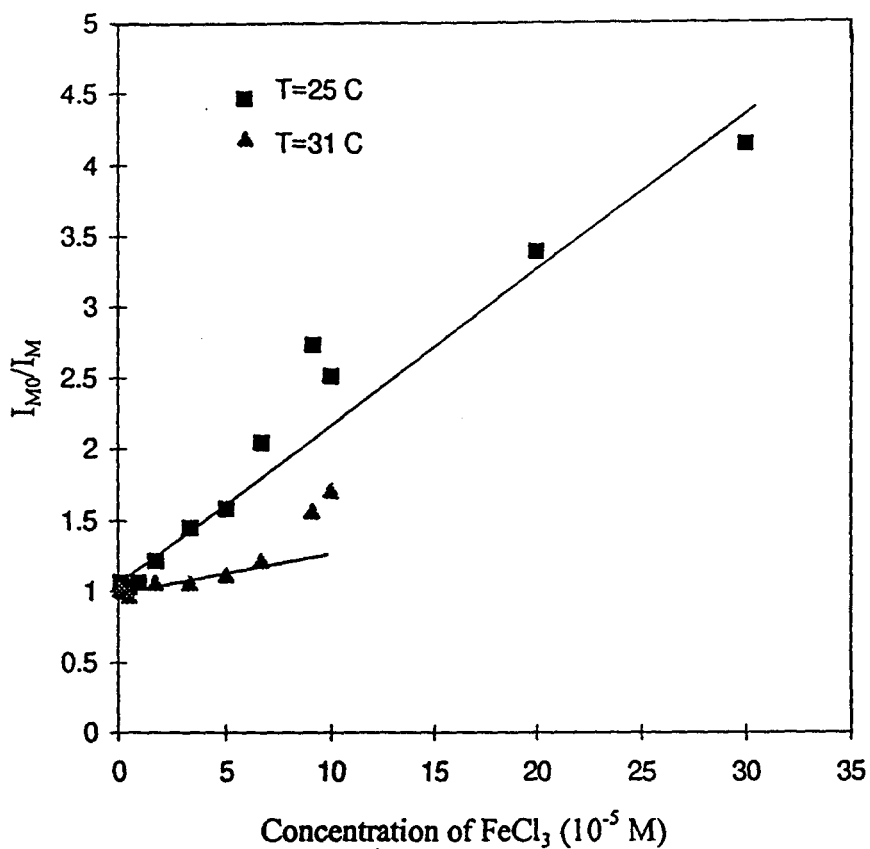
Figure 16: Ratio of I_0/I pyrene monomer emission intensities in the absence and in the presence of $FeCl_3$ in PNIPAM/NAV/Py-an aqueous solutions as a function of $FeCl_3$ concentrations at temperature 25 and 31°C, polymer concentration 0.05g/l, λ_{exc} = 346nm.
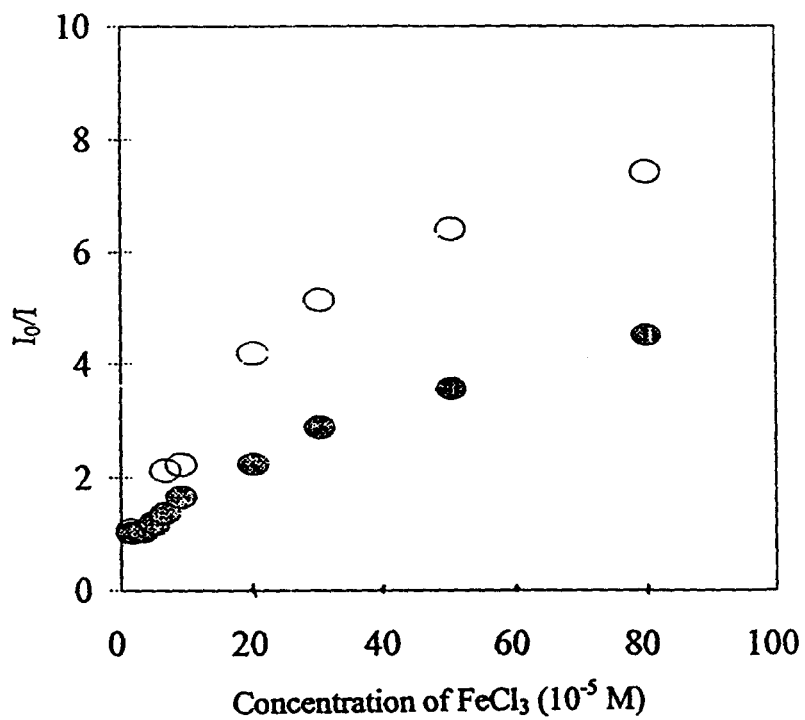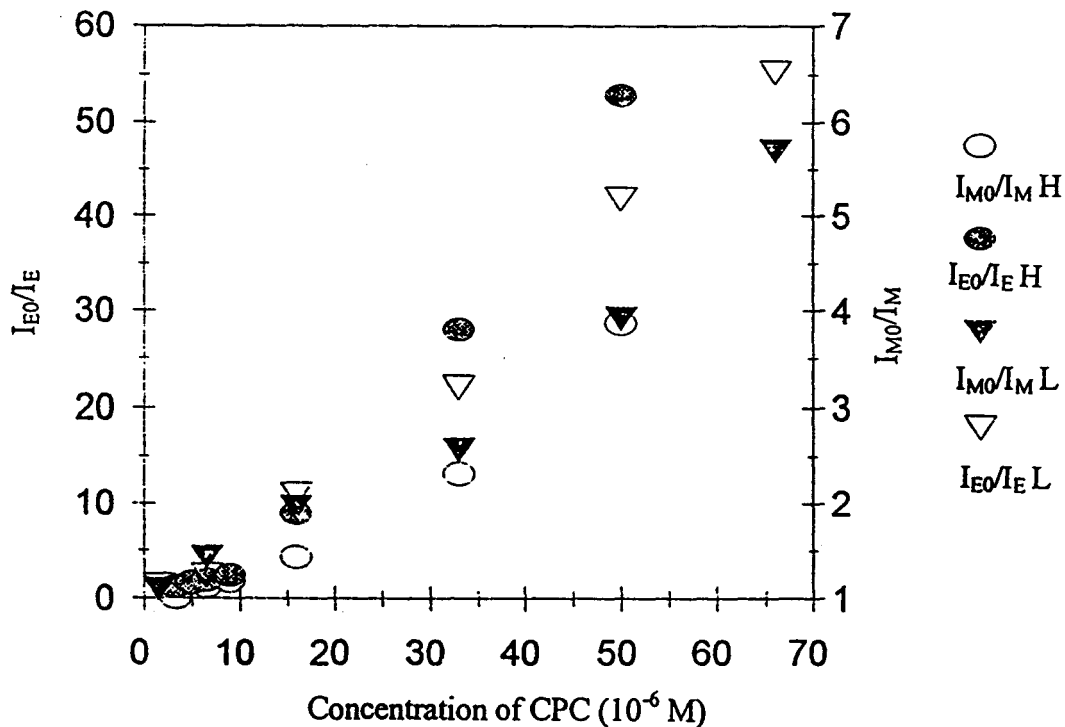
Figure 17: Ratio of I_0/I pyrene monomer emission intensities (solid circle) and excimer emission intensities (circle) in the absence and in the presence of FeCl$_3$ in PNIPAM/NAV/Py-ad aqueous solutions as a function of FeCl$_3$ concentrations, polymer concentration 0.05g/l, 25°C, λ_{exc} = 346nm.

.

Figure 18 : Ratio of I_0/I pyrene monomer emission intensities (solid circle) and excimer emission intensities (circle) in the absence and in the presence of NaI in copolymer aqueous solutions as a function of NaI concentrations, polymer concentration 0.05g/l, 0.005g/l, 25°C. a).PNIPAM/NAV/Py-ad, λ_{exc} = 346nm. b) PNIPAM/NAV/Py-an, λ_{exc} = 344nm;

Figure19: Ratio of I_0/I pyrene monomer emission intensities in the absence and in the presence of NaI in PNIPAM/NAV/Py-ad buffer solutions as a function of NaI concentrations, polymer concentration 0.05g/l, B: pH=9, W: Water, A: pH=2.5, 25°C. λ_{exc} = 346nm.

Figure 20: Ratio of I_0/I pyrene monomer emission intensities (I_{m0}/I_m) and excimer emission intensities (I_{E0}/I_E) in the absence and in the presence of cetylpyridinium chloride (CPC) in PNIPAM/NAV/Py-ad buffer solutions as a function of CPC concentrations, polymer concentration 0.05g/l and 0.005g/l, 25°C, $\lambda_{exc} = 346$nm.

Figure 21: Ratio of I_0/I pyrene monomer emission intensities (I_{m0}/I_m) and excimer emission intensities (I_{E0}/I_E) in the absence and in the presence of cetylpyridinium chloride (CPC) in PNIPAM/NAV/Py-an buffer solutions as a function of CPC concentrations, polymer concentration 0.05g/l and 0.005g/l, 25°C, λ_{exc} = 344nm.
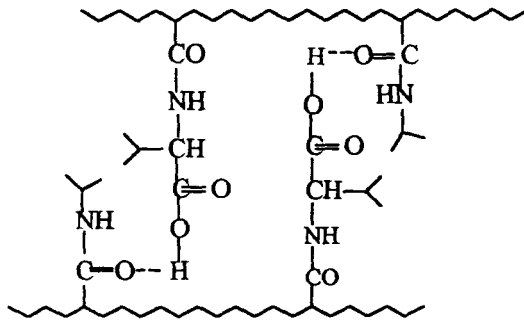
many bonds in acidic conditions -no mobility
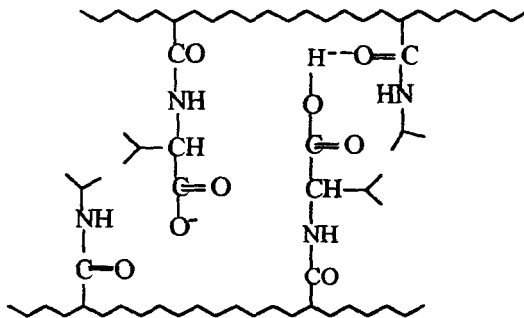
Increasing mobility with pH increase
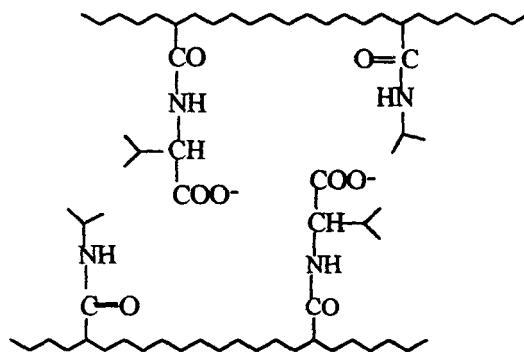
No bonding in basic conditions

Diagram 4 Complexation between amide and carboxylic groups in buffers
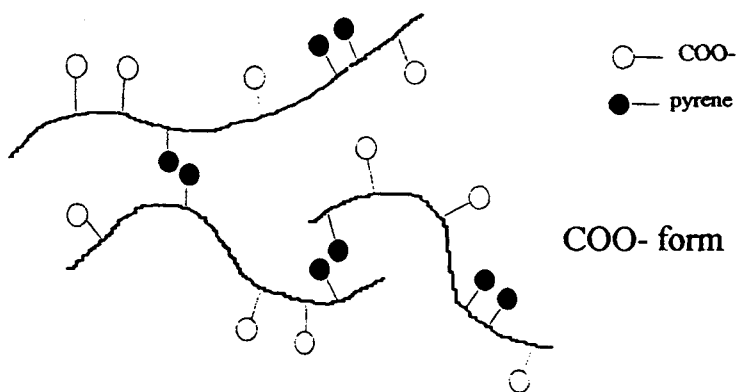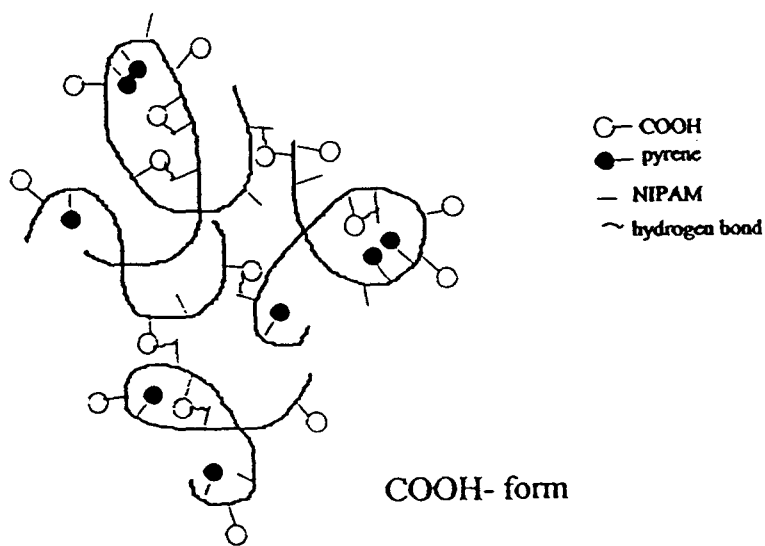
Diagram 5 Conformations of PNIPAM/NAV/Py-ad in buffers
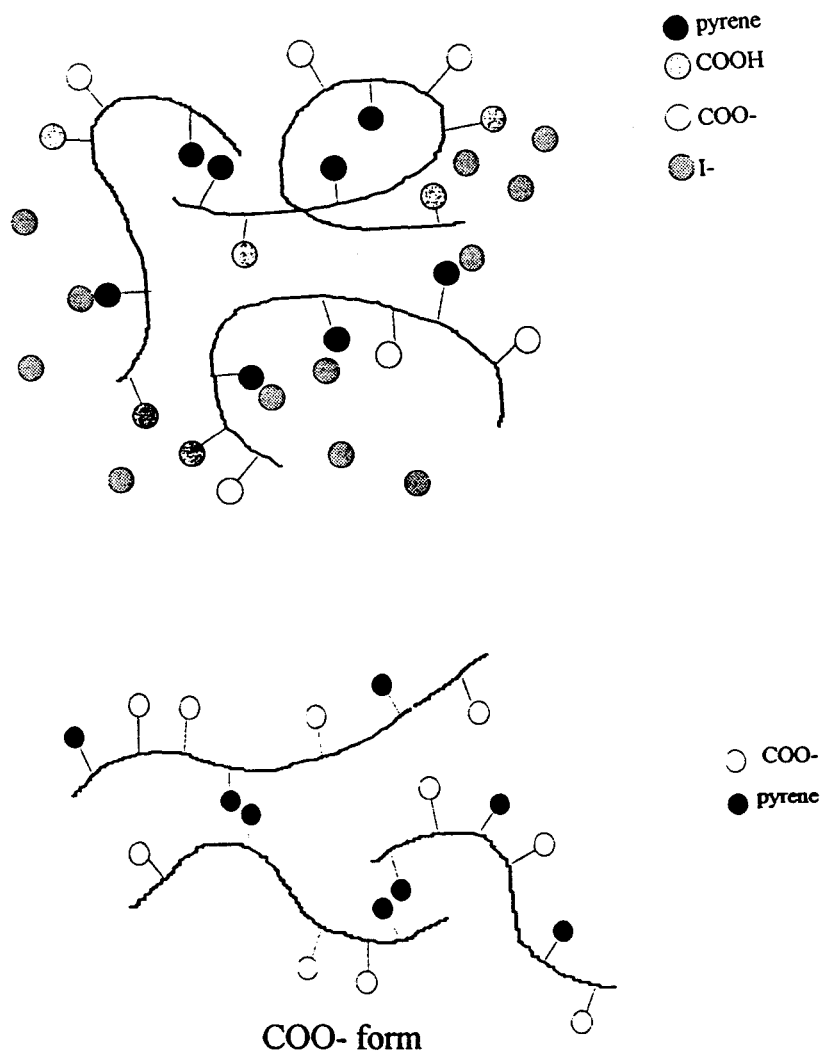
pyrene

◯ COOH

◖ COO-

◉ I-

◖ COO-

● pyrene

COO- form

Diagram 6 Conformations of PNIPAM/NAV/Py-an in Buffers

● pyrene

⊛ COOH

○ COO-

● Fe3+

a) PNIPAM/NAV/Py-an

● pyrene

◉ COOH

◡ COO-

● Fe3+
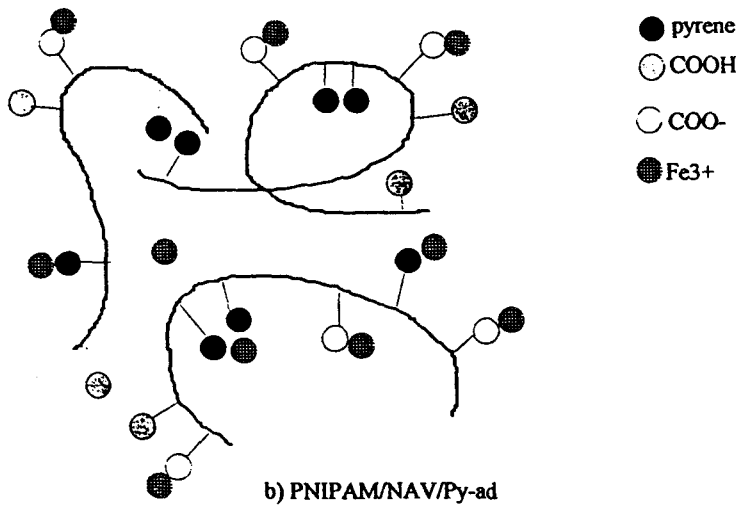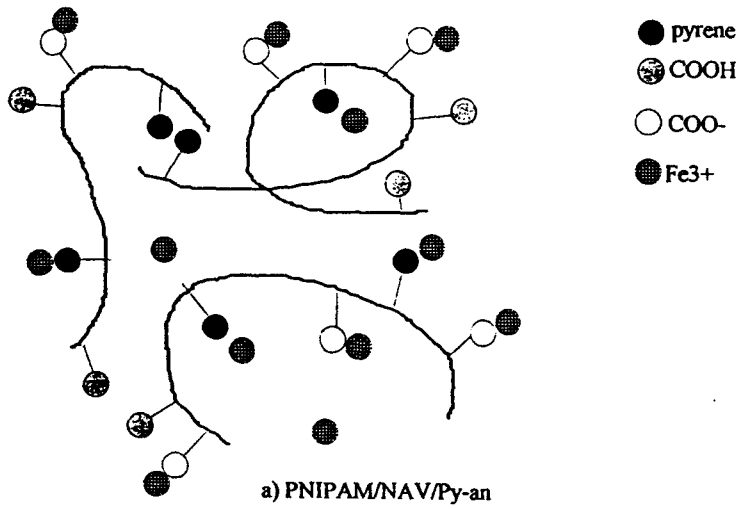
b) PNIPAM/NAV/Py-ad

Diagram 7 Polymer Quenched by Fe3+ in Water

104
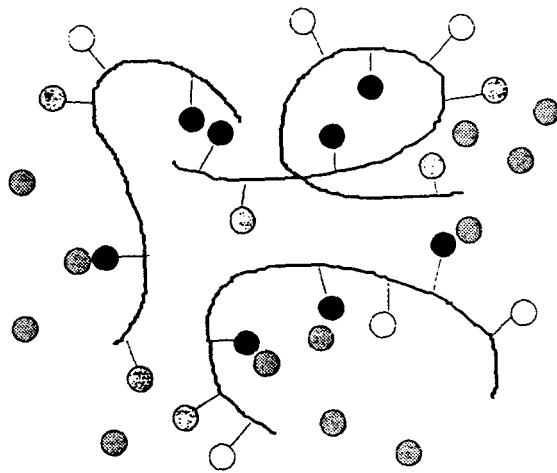
b) PNIPAM/NAV/Py-an

b) PNIPAM/NAV/Py-ad

- ● pyrene
- ⊛ COOH
- ○ COO-
- ⊛ I-

Diagram 8 Polymer Quenched by I- in Water